applied sciences

MDPI

Article

Comparative Study on the Synthesis of Path-Generating Four-Bar Linkages Using Metaheuristic Optimization Algorithms

Yaw-Hong Kang [1,*], Jau-Wen Lin [1] and Wei-Chen You [2]

[1] Department of Mechanical Engineering, National Kaohsiung University of Science and Technology, Kaohsiung City 80778, Taiwan; denis@nkust.edu.tw
[2] Kwang Yang Motor Co., Ltd., Kaohsiung City 80794, Taiwan; kk940614@hotmail.com
* Correspondence: yhkang@nkust.edu.tw

Abstract: Four-bar linkages are one of the most widely used mechanisms in industries. This paper presents a comparative study on the accuracy and efficiency of the optimum synthesis of path-generating four-bar linkages using five metaheuristic optimization algorithms. The utilized metaheuristic methods included two swarm intelligence-based algorithms, i.e., particle swarm optimization and hybrid particle swarm optimization, and three evolutionary-based algorithms, i.e., differential evolution, ensemble of parameters and mutation strategies in differential evolution, and linearly ensemble of parameters and mutation strategies in differential evolution. The objective function to be minimized is the sum of squares of the distance between the generated points and the precision points of a coupler point. The optimal design of four-bar linkages must meet the Grashof's criteria and exhibit sequential constraints that can prevent the occurrence of order defect. This study investigated five representative cases of the dimensional synthesis of four-bar path generators with and without prescribed timing and compared the optimal solutions of the utilized five metaheuristic methods to those of previously reported algorithms in literature. The improved metaheuristic methods exhibited superior optimal solution and enhanced reliability compared to the original methods. Moreover, three improved metaheuristic methods were not only easy implemented, but also more efficient for solving the optimal synthesis problems, particularly for high dimensional problems.

Keywords: path-generating four-bar linkage; metaheuristic optimization algorithm; swarm intelligence-based algorithm; evolutionary-based algorithm

Citation: Kang, Y.-H.; Lin, J.-W.; You, W.-C. Comparative Study on the Synthesis of Path-Generating Four-Bar Linkages Using Metaheuristic Optimization Algorithms. *Appl. Sci.* **2022**, *12*, 7368. https://doi.org/10.3390/app12157368

Academic Editor: Vincent A. Cicirello

Received: 28 June 2022
Accepted: 19 July 2022
Published: 22 July 2022

1. Introduction

A planar four-bar linkage is an important mechanism that is widely employed in industrial applications. For example, path-generating four-bar linkages (or four-bar path generators) are applied in thread pick-up mechanisms in sewing machines [1], agricultural rice seeding transplanting mechanisms [2], human gait rehabilitation systems [3] and knee exoskeletons [4], underwater manipulators [5], and in robotic fingers [6]. The synthesis problems of linkages can be categorized into three types [7]: (1) type synthesis, (2) number synthesis, and (3) dimensional synthesis. The dimensional synthesis problem involves the determination of the dimensional or geometric size of mechanisms, such as lengths, angles, initial motion position, and coordinates of the pivot, to ensure that the designed mechanisms can meet the required motion. The dimensional synthesis problems of mechanisms can be classified into function generation, path generation, and motion generation. The dimensional synthesis of path-generating four-bar linkages (termed as path synthesis problem in this work) involves the design of the parameters of a mechanism to ensure that the coupler point traces the desired path defined by a number of precision points, which is the central work of this research, and it is also a classical problem that has been investigated by numerous researchers for several decades, and some papers have reviewed the path synthesis problems [8–10]. Traditionally, the synthesis of such problems is solved using

graphical methods [11], analytical methods [7], numerical methods [12,13], and a combined numerical and analytical method [14]. However, owing to the limitations of the number of precision points (the maximum precision points for the synthesis of four-bar path generation problem is nine), the solutions of path synthesis problems should address complex non-linear equation under constraints, which cannot be easily solved using traditional methods. With the rapid development of diverse optimization techniques, determining the fittest value through efficient numerical calculations has emerged as a major trend. This is because numerical calculations can rapidly search for the best design parameters within the design constraints, thus effectively reducing the calculation time and the converging rate to optimal solutions. Commonly used optimization methods can be divided into two main categories. The first category includes traditional gradient-based methods that require the determination of the derivative of the objective function, such as the Guass–Newton method [15], the gradient method [16–20], tabu-gradient method [21], ant-gradient method [22–24], and the sequential quadratic programming (SQP) method [25]. However, these methods cannot easily determine the function derivative when dealing with complex problems with nonlinear implicit objective functions. The second category includes free-derivative and population-based metaheuristic global optimization methods, which consist of two important groups. The first group includes the swarm intelligence-based algorithms inspired by biological swarm behavior, including the well-known particle swarm optimization (PSO) algorithm [26], cuckoo search (CS) algorithm [27], krill herd (KH) algorithm [28], and their improved variants. The second group includes the evolutionary-based algorithms inspired by biological evolution, including the well-known genetic algorithm (GA) [29], differential evolution (DE) algorithm [30], imperialist competitive algorithm (ICA) [31], teaching learning-based optimization (TLBO) algorithm [32], and their improved variants. For a comparative study comparing other optimal solutions reported in previous literature, here, we briefly review the metaheuristic global optimization methods and other methods applied to the optimal path synthesis problems.

(1) Swarm intelligence-based algorithms:

These methods include PSO, HPSO, MKH, CS, APT-FPSO, BAS, etc. Kang et al. [33] proposed a hybrid PSO method (HPSO) to solve optimal path synthesis problems with and without prescribed timing, and verified the superiority of HPSO to PSO and DE. Bulatovic et al. [34] proposed a modified krill herd (MKH) algorithm for the dimensional synthesis problems of a four-bar path generator, and confirmed the efficiency of the proposed method on four benchmark tested examples. Lin et al. [35] employed two population-based metaheuristic optimization methods, cuckoo search (CS) and TLBO algorithms, to solve five representative problems and found that CS exhibited superior accuracy and exploitation capacity to DE and TLBO. Sadeghi et al. [36] employed an adaptive particularly tunable fuzzy PSO (APT-FPSO) algorithm to solve the optimum path synthesis problem of defect-free four-bar mechanisms. Mo et al. [37] applied a new metaheuristic algorithm, known as the beetle antennae search (BAS) algorithm, to solve the path and function synthesis problems of four-bar and Stephenson-III six-bar mechanisms. Eight examples with and without prescribed timing were investigated, and the optimal results demonstrated that the BAS method outperformed GA, PSO, and DE methods.

(2) Evolutionary-based algorithms:

These methods include GA, GA-KK, GA-CSP, DE, GA-FL, GA-DE, MUMSA, NSGA-II, IOA$^{s\text{-}at}$, ICA-SA, DE-SRT, TS-MBFOA, SAP-TLBO, ICA-GA, TLBO, CMDE, CPF-DE, multi-start, HLIDE, ADELI, DEC, ImHS, GSA, ATLBO-DA, GSEF-IAA, ODSRA + CP, REA, HCDJ, etc. Connor et al. [38] applied a genetic algorithm (GA) to solve optimal path synthesis problems. Kunjur et al. [39] presented a GA-based approach (GA-KK) for solving optimal path synthesis problems with prescribed timing. Zhou et al. [40] presented an objective function based on the orientation structural error of the fixed link of a crank-rocker path generating linkage, and applied GA to determine the optimal solutions. Cabrera et al. [41] presented a GA-based algorithm (GA-CSP) for the

optimal synthesis of path-generating four-bar linkages. Shiakolas et al. [42] applied DE method and a technique known as the geometric centroid of precision points to solve optimal path synthesis problems with prescribed timing. Laribi et al. [43] proposed a combined GA-fuzzy logic (GA-FL) method to solve optimal path synthesis problems. Nariman-Zadeh et al. [44] employed a hybrid multi-objective GA for the Pareto synthesis of a path-generating four-bar linkage, considering the simultaneous minimizations of two conflicting objective functions (tracking error and transmission angle error). Bulatovic et al. [45] applied a DE algorithm and variable controlled deviations method to synthesize a Grashof four-bar linkage with the motion of a coupler point along a large number of points on a straight line. Acharyya et al. [46] applied three metaheuristic optimization algorithms, GA, PSO, and DE algorithms, for the optimal synthesis of a path-generating four-bar linkage, and compared the performance of the three algorithms, finding that the DE method exhibited the best performance. Lin [47] proposed a GA-DE hybrid evolutionary algorithm for the optimum synthesis of a four-bar path generator, and replaced the GA with an improved difference vector, which can effectively retain better individuals during the crossover operation of the GA, thus improving the efficiency and accuracy of the solution. Cabrera et al. [48] proposed an evolutionary algorithm, named MUMSA, which utilizes mutation steps to make the result closer to the global optimal solution for the optimum synthesis of a path-generating four-bar mechanism. Peñuñuri et al. [49] applied a DE algorithm to perform the optimal synthesis of hybrid-task and path generation of four-bar linkages with and without prescribed timing. Khorshidi et al. [50] considered the tracking error of a mechanism, the deviation of its transmission angle from 90°, and the maximum angular velocity ratio as the multi-objectives of an optimization problem, and employed a hybrid Pareto GA with a built-in adaptive local search to optimally design a path-generating four-bar linkage. Matekar et al. [51] proposed a modified error function and employed a DE algorithm to solve the optimal path synthesis problems. Badduri et al. [52] proposed a GA-based method, named the NSGA-II method, for the optimal coupler-curve synthesis of a planar four-bar linkage. Ortiz et al. [53] proposed a DE-based algorithm, called Ingeniería Mecánica Málaga (IMMa) optimization algorithm with self-adaptive control parameters technique, IOA$^{s\text{-}at}$, to solve the dimensional synthesis problems of five cases of four-bar and one case of six-bar path-generating mechanisms. Lin [54] proposed a two-phase synthesis method in which the first phase involves shape optimization followed by a scale-rotation-translation (SRT) synthesis optimization for the synthesis of path-generating four-bar mechanisms. Next, Lin employed a GA-DE evolutionary algorithm to solve the optimal synthesis problem, and two representative cases were investigated to verify the higher accuracy of the solutions achieved by the proposed method. Ebrahimi et al. [55] utilized an imperialist competitive algorithm (ICA) along with a parallel simulated annealing (SA) algorithm, called the ICA-SA method, for the dimensional synthesis of path-generating four-bar mechanisms with and without prescribed timing, and compared the performance of the algorithms to those of some other heuristic algorithms (GA, DE, and PSO). Lin et al. [56] proposed a one-phase synthesis method without using the input angles as a design variable for optimum path synthesis problems, and employed a DE algorithm with an SRT technique (DE-SRT) to improve the solution reliability and accuracy. Hernandez-Ocana et al. [57] included two-swim operators to the chemotaxis process of the modified bacterial foraging optimization algorithm (TS-MBFOA), an evolutionary-based algorithm, to solve the optimal synthesis problems of path-generating four-bar mechanisms. Sleesongsom et al. [58] proposed a self-adaptive population size TLBO (SAP-TLBO) algorithm for the optimal path synthesis of a four-bar linkage. Two traditional path generation test problems were conducted, and the optimum results revealed the superiority of the SAP-TLBO algorithm compared to original TLBO method. Mohamed et al. [59] simultaneously considered three conflicting objective functions, which are the tracking error, the deviation of the transmission angle from 90°, and the maximum angular velocity ratio, as a multi-objective function for the optimal synthesis of four-bar mechanisms using an ICA coupled with a GA (ICA-GA).

Lin et al. [60] proposed a combined mutation differential evolution (CMDE) algorithm for the optimum synthesis of path-generating four-bar mechanisms. The combined strategies of the mutations: are DE/best/1, DE/current-to-best/1, and DE/rand/1. The enhanced population diversity and search effectiveness of the CMDE algorithm compared to DE was demonstrated using five representative problems. Kafash et al. [61] introduced an objective function called circular proximity function (CPF), which exhibits the lowest number of optimization variables, and DE, called the CPF-DE method, to solve the optimal path synthesis problems. Singh et al. [62] proposed a TLBO algorithm to solve the optimal synthesis problems of human knee exoskeletons and a crank-rocker four-bar path generating linkage. Buskiewicz et al. [63] presented a one-phase synthesis method that can reduce the number of design parameters for the optimal synthesis of a four-bar mechanism generating open/closed paths with prescribed timing. Three cases were investigated using a DE algorithm to validate the effectiveness of the method. Sleesongsom et al. [64] applied a TLBO method with a constraint-handling technique, named a path-repairing technique, to address the constraints of both input crank rotation and Grashof's criterion, and some metaheuristic algorithms, including ABC, JADE, PBIL, ACOR, SCA, GWO, and TLBO, were applied to determine the optimum solutions of path-generating four-bar linkages. Three representative cases were investigated, and the optimum results revealed that TLBO outperformed the other methods. Based on the optimal trajectory tracking control theory of a shadow robot, Sabaapour et al. [65] proposed a contour-error-based proportional-derivative objective function for synthesizing path-generating four-bar mechanisms, and employed a global optimization method, known as the multi-start heuristic algorithm, to solve the optimal synthesis problem. Zhang et al. [66] presented a hybrid Lagrange interpolation differential evolution (HLIDE) algorithm to enhance the local exploitation capability of DE for optimal synthesis problems. Five cases of optimal four-bar path generating linkages were tested and compared to those of three evolutionary algorithms (PSO, TLBO, and DE), and the results demonstrated the significantly enhanced performance of HLIDE compared to those of the other algorithms. Huang et al. [67] presented an adaptive DE, and incorporated a local search with the Lagrange interpolation argument algorithm (ADELI) to enhance the exploitation capability of DE. Thirty benchmark function sets in the CEC 2014 were tested to verify the feasibility and effectiveness of ADELI, and a synthesis problem of a path-generating four-bar linkage with prescribed timing was optimized. Romero et al. [68] proposed a robust objective function formulation based on natural coordinates and the Hermitian conjugate operator, and implemented a modified TLBO algorithm for the optimal synthesis of a four-bar path generator. Sancibrian et al. [69] proposed a search procedure for the optimal solution of the dimensional synthesis of planar linkages by hybridizing a local search approach (generalized reduced gradient method) and DE. They compared three hybrid strategies and verified that the cluster-based hybridization in DE (DEC) is the best hybrid approach. Flores-Pulido et al. [70] proposed an improved harmony search (ImHS) algorithm to solve the dimensional synthesis problems of a four-bar path generator without prescribed timing. Zarkandi [71] proposed a population-based heuristic algorithm called a gravitational search algorithm (GSA) to determine multiple cognate- and defect-free optimal solutions for the path synthesis problems of planar four-bar and slider-crank mechanisms. Zhang et al. [72] presented an error feedback method (EFM) for linear constraint optimization problems. They optimized two path-generating four-bar linkages using DE, PSO, and TLBO methods, and the objective function with linear inequality constraints was optimized using the penalty function method and EFM. The experimental results revealed that EFM exhibited significantly enhanced stability and faster convergence than the traditional penalty function method. Bureerat et al. [73] proposed a new constraint handling technique which deals with both input crank rotation and Grashof's criterion for the synthesis of path-generating four-bar linkages. In addition, they solved several optimization problems using a new adaptive TLBO with a diversity archive (ATLBO-DA) algorithm. Sardashti et al. [74] proposed a new objective function, the geometrical similarity error function (GSEF), and applied an innovative adaptive algorithm

(IAA) operator to form the GSEF-IAA methodology for the synthesis problem of a path-generating four-bar mechanism. Valencia-Segura et al. [75] applied a differential evolution variant (DE/best/1/bin) to solve the optimal dimensional synthesis of a four-bar path generation mechanism using a relative angle and the Cartesian space link parameterization (ODSRA + CP) method. Five study cases of dimensional synthesis for path generation with and without prescribed timing were solved and comparatively studied with the well-known vector loop-based synthesis method, and were solved by metaheuristic algorithms. Huang et al. [76] proposed a repellency evolutionary algorithm (REA) to solve the dimensional synthesis of path-generating four-bar mechanisms. The REA consists of two repulsive mutation behaviors, which exhibit two common characteristics: (i) the population no longer learns from the current global optimum to prevent the population from falling into the local optimum region; (ii) the offspring searches any direction except the location of the parent. Sy et al. [77] proposed a hybrid-combined differential evolution and Jaya (HCDJ) algorithm, which uses a modified initialization, a hybrid-combined mutation between the DE and Jaya algorithm, and an elitist selection for the dimensional synthesis of path-generating four-bar mechanisms with symmetrical motions. Five representative problems were tested, and the HCDJ algorithm was confirmed to provide an improved optimal solution than the original DE and Jaya methods and some algorithms presented in the literature. Yao et al. [78] developed a new constraint-handling method called the individual repairing (IR) method as an alternative to the penalty function method and applied three metaheuristic methods (GA, DE, and PSO) for the optimal synthesis of path-generating four-bar linkages. Two cases with prescribed timing and one case without prescribed timing were tested to verify the reliability of the IR method, and the results revealed that the optimal solutions of the IR method are superior to those of the algorithms proposed by Acharyya et al. [46].

(3) Path-based synthesis methods:

These methods include the Fourier descriptors (FDs) method and Haar wavelet transform method. McGarva [79] employed the harmonic analysis method and normalization technique to create a library of path generation mechanisms of variable types to be generated and stored in terms of the normalized Fourier coefficients (NFCs) of the path they generate. Ullah et al. [80] proposed an objective function based on FDs that evaluates only the shape difference between desired and candidate coupler curves for an optimal synthesis problem. The FDs method has the ability to decouple the nine design variables involved in path generation problem, and Ullah et al. [80] first applied the FDs method to reduce the dimension of the search space from nine to five. Vasiliu et al. [81] presented a case-based approach using neural networks to synthesize the dimensions of planar four-bar path generators, in which the shape of the desired path was represented using normalized FDs. Liu et al. [82] proposed a refined numerical representation (RNR) method to describe the shape character of path curves and define the objective function of the optimum path synthesis problems. In addition, they determined the possible solutions using the artificial immune network global searching (AIS) method. Starosta [83] utilized NFCs to represent a closed curve, and employed GA, named the GA-FC method, for the synthesis of a four-bar path generator. Galán-Marín et al. [84] developed a wavelet-based neural network method to describe the close path shape and optimally synthesize crank-rocker path-generating linkages. Buskiewicz et al. [85] utilized the NFCs of a curve curvature as a curve description for the optimal synthesis of a path mechanism. In their work, the distance norm between two curves was considered as the distance between their NFCs, which was used as the objective function, and GA was applied for the optimal path synthesis problems. Khan et al. [86] proposed an approach where artificial neural networks (ANNs) were used to establish a relationship between the FDs of a desired coupler curve and the corresponding dimensions of a four-bar linkage. Sun et al. [87] presented a synthesis method for the open path generation of a four-bar mechanism using the Haar wavelet transform and normalization to extract the wavelet output feature parameters (WOFP) of an open path. Lin et al. [88] presented a parametrization-invariant FD-based method for the optimal synthesis of a path-generating four-bar mechanism. In addition, they determined the optimal

values of the design parameters using a back propagation (BP) neural network algorithm. Sharma et al. [89] proposed a non-uniform FD-based path synthesis algorithm with an optimal parameterization scheme for a path-generating four-bar mechanism and determined the optimal solution using the Nelder–Mead simplex optimization method. Kim et al. [90] proposed a two-step optimization methodology for path-generating, crank-rocker four-bar linkages based on first-order and second-order derivations of a specified coupler curve, and a hybrid Taguchi-random coordinate search algorithm (HTRCA), which is an experimental-based and free-derivative method, was applied to minimize the objective function (the root mean square error) with the reference slope and its change in the angle of the slope. Kim et al. [91] applied the HTRCA method to synthesize three cases of path-generating four-bar linkages with and without prescribed timing. They compared the optimal results of the HTRCA method with those of some evolutionary algorithms (GA-CSP, GA, PSO, DE, and GA-DE) to verify the robustness and efficiency of the HTRCA method. Li et al. [92] presented an analytical approach for four-bar path generation synthesis based on the FCs of the path, named the Anal-FC method. Based on the Anal-FC method, the synthesis problem was reduced to solving two polynomial equations without any limitation on the number of the precision point.

(4) Other optimization methods:

Ahmadi et al. [93] applied a Stackelberg game-theoretic approach for the multi-objective optimal synthesis of path-generating four-bar mechanisms. The tracking error and the deviation of the transmission angle from 90° were considered as the bi-objective function. Ahmadi et al. [94] proposed an approach based on the synergy of cooperative game theory, reliability-based design optimization (RBDO), and Monte Carlo simulation (MCS), called RBDO-MCS method, to solve the problem of the multi-objective optimal synthesis of path-generating four-bar mechanisms. In the approach, three performance criteria: tracking error, deviation of the transmission angle from 90°, and probability of failure of Grashof's constraint, were considered as the three objective functions.

Owing to the random search characteristics of the optimization methods, the efficiency (or effectiveness) and accuracy are significantly affected by the selected parameters of the algorithms, such as the number of populations, crossover ratio, scale factor, and iterative number used in the method. The obtained optimization results may differ at each time; thus, effectively determining the performance of an optimization algorithm is a critical problem. To find accurate and efficient global optimization algorithms for solving high dimensional synthesis problems, such as the synthesis of a six-bar or eight-bar path-generating linkage, is the intent of this preliminary study. In previous research on optimization methods, comparison tests were often performed based on some benchmark functions or representative problems, and the statistical mean value and standard deviation (SD) were applied to judge the merits of the methods. In this study, five metaheuristic global optimization methods were applied to solve five representative optimization problems in the dimensional synthesis of path-generating four-bar linkages, in which two of these methods include a widely used intelligent algorithm and evolutionary algorithm (i.e., PSO and DE methods), and three of these methods are improved PSO- and DE-based methods (i.e., hybrid PSO (HPSO) [33], ensemble of parameters and mutation strategies in differential evolution (EPSDE) [95], and linearly EPSDE (L-EPSDE) method). The HPSO, EPSDE, and L-EPSDE methods would be verified to be suitable for application in middle or high dimensional problems. In this study, one hundred trials of optimization design were investigated to solve each case of the five representative synthesis problems. The accuracy and efficiency (effectiveness) of these five metaheuristic optimization methods were compared; moreover, they were also compared to those of previously reported algorithms in the literature. The comparative results revealed that the accuracy and efficiency of the adaptive improved methods, EPSDE and L-EPSDE, are superior to numerous previously reported methods, and that they are suitable for application in middle or high dimensional problems, and that DE with golden ratio (DE-gr) also exhibited a similar outperforming characteristic as EPSDE and L-EPSDE in middle dimensional problems. In addition, HPSO

exhibited improved accuracy and efficiency compared to the original PSO, and is suitable for application in middle or high dimensional problems.

The remainder of this paper is organized as follows: Section 2 presents the formulation of the synthesis problem of a path-generating four-bar linkage. Section 3 briefly describes the five metaheuristic global optimization algorithms employed in this study. Section 4 presents the application of the five metaheuristic optimization algorithms for solving five representative problems of a four-bar path generator and the comparative study of the performance of the algorithms to those of previously reported algorithms. Section 5 briefly discusses the overall optimal results of the five metaheuristic optimization methods. Lastly, the conclusion is drawn in Section 6.

2. Position Analysis of the Planar Four-Bar Linkage

Figure 1 shows the vector loop diagram of the planar path generating four-bar linkage [49], where r_1 is the length of fixed link, r_2 is the length of input link, r_3 is the length of the coupler link, r_4 is the length of output link, and r_{cx} and r_{cy} are the projection and normal distance of the coupler point C to the line connecting joint A and joint B, respectively. Angle θ_0 is the inclined angle of the fixed link on the horizontal axis, and (x_0, y_0) is the coordinate of the fixed pivot O of the mechanism on the X–Y coordinate system.

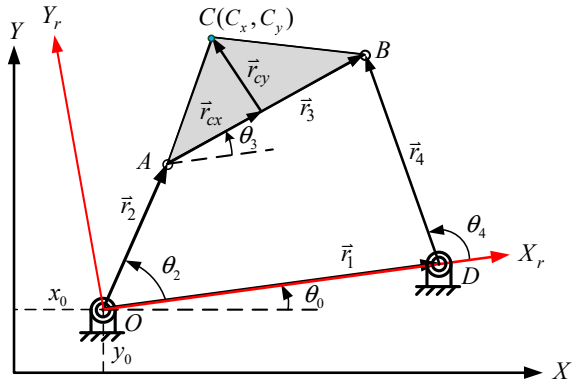

Figure 1. Vector loop diagram of a planar path-generating four-bar linkage.

From the vector loop defined on the planar four-bar linkage, we obtain:

$$\vec{r_3} = \vec{r_1} + \vec{r_4} - \vec{r_2} \tag{1}$$

By taking the inner product of its own vector:

$$\vec{r_3} \cdot \vec{r_3} = (\vec{r_1} + \vec{r_4} - \vec{r_2}) \cdot (\vec{r_1} + \vec{r_4} - \vec{r_2}) \tag{2}$$

The above equation can be expanded to:

$$r_3{}^2 = r_1{}^2 + r_4{}^2 + r_2{}^2 + 2r_1r_4\cos\theta_4 - 2r_1r_2\cos\theta_2 - 2r_2r_4\cos(\theta_2 - \theta_4) \tag{3}$$

After expanding the trigonometric function, we obtain:

$$A\cos\theta_4 + B\sin\theta_4 = C \tag{4}$$

where

$$\begin{aligned} A &= 2r_4(r_1 - r_2\cos\theta_2) \\ B &= -2r_2r_4\sin\theta_2 \\ C &= r_3{}^2 - r_1{}^2 - r_2{}^2 - r_4{}^2 + 2r_1r_2\cos\theta_2 \end{aligned} \tag{5}$$

Using the half-angle formula of tanθ we derive:

$$(C + A)\tan^2(\frac{\theta_4}{2}) - 2B\tan(\frac{\theta_4}{2}) + (C - A) = 0 \quad (6)$$

By solving for θ_4

$$\theta_4 = 2\tan^{-1}\left[\frac{B \pm \sqrt{A^2 + B^2 - C^2}}{A + C}\right] \quad (7)$$

By decomposing Equation (1) into the x–y components, θ_3 can be solved and expressed as:

$$\theta_3 = \tan^{-1}\left(\frac{r_4\sin\theta_4 - r_2\sin\theta_2}{r_1 + r_4\cos\theta_4 - r_2\cos\theta_2}\right) \quad (8)$$

The coordinate components of the coupler point C on the Xr–Yr coordinate system, (C_{xr}, C_{yr}), can be expressed as

$$\begin{cases} C_{xr} = r_2\cos\theta_2 + r_{cx}\cos\theta_3 - r_{cy}\sin\theta_3 \\ C_{yr} = r_2\sin\theta_2 + r_{cx}\sin\theta_3 + r_{cy}\cos\theta_3 \end{cases} \quad (9)$$

The trajectory of the coupler point C on the X–Y coordinate system,(C_x, C_y), can be expressed as

$$\begin{bmatrix} C_x \\ C_y \end{bmatrix} = \begin{bmatrix} \cos\theta_0 & -\sin\theta_0 \\ \sin\theta_0 & \cos\theta_0 \end{bmatrix}\begin{bmatrix} C_{xr} \\ C_{yr} \end{bmatrix} + \begin{bmatrix} x_0 \\ y_0 \end{bmatrix} \quad (10)$$

3. Optimization Methods

3.1. Particle Swarm Optimization and Hybrid Particle Swarm Optimization Methods

The particle swarm optimization (PSO) method was proposed by Kennedy and Eberhart in 1995 [26], and it employs the social behavior of birds or fish when searching for food as the searching solution concept of the optimization method. Particles correspond to an individual in a school of birds or fish: when a flock of bird searches for food, the moving velocity and direction of each individual are affected by three factors, namely inertial velocity, individual experience, and group influence. Inertial velocity refers to the flying velocity of birds during search, and it affects the search direction and velocity of an individual. Individual experience refers to the accurate direction and velocity of an individual based on past experience. Group influence refers to the effect of the group behavior on individuals, and individuals move toward the individual closest to the food at the moment. In the D-dimensional search space, each particle exhibits a position vector $\mathbf{x}_i = (x_{i1}, x_{i2}, \ldots, x_{i\,D})$ with a velocity vector $\mathbf{v}_i = (v_{i1}, v_{i2}, \ldots, v_{i\,D})$. Particles are originally initialized in a uniform random manner through the search space, and the velocity is also randomly initialized. The new position (x_i^{i+1}) and new velocity (v_i^{i+1}) of each particle movement are as follows.

$$v_i^{t+1} = v_i^t + c_1 \times rand(\,) \times (P_i^t - x_i^t) + c_2 \times Rand(\,) \times \left(P_g^t - x_i^t\right) \quad (11)$$

$$\begin{aligned} x_i^{t+1} &= x_i^t + v_i^{t+1} \\ -V_{\max} &\le v_i^t \le V_{\max} \end{aligned} \quad (12)$$

where i corresponds to each individual, t is the number of iterations (generations), x_i^t is the position of an individual, v_i^t is the velocity of an individual, P_i^t is the best position (*Pbest*) of an individual i at t-th iteration, P_g^t is the global best position (*Gbest*) of the swarm at t-th iteration, c_1 and c_2 are the acceleration coefficients or learning factors, and they represent the cognitive and social component, respectively, and are used to decide whether particles prefer moving toward a *Pbest* position or *Gbest* position. Most studies utilize learning factors of 2, which indicates that the same importance is given to cognitive searching and social searching; $rand(\,)$ and $Rand(\,)$ are two uniformly distributed random numbers between

0 and 1. The drawbacks of the original PSO method is the requirement for specifying the velocity v_i^t within $[-V\max, V\max]$. The flow chart of the PSO algorithm is shown in Figure 2.

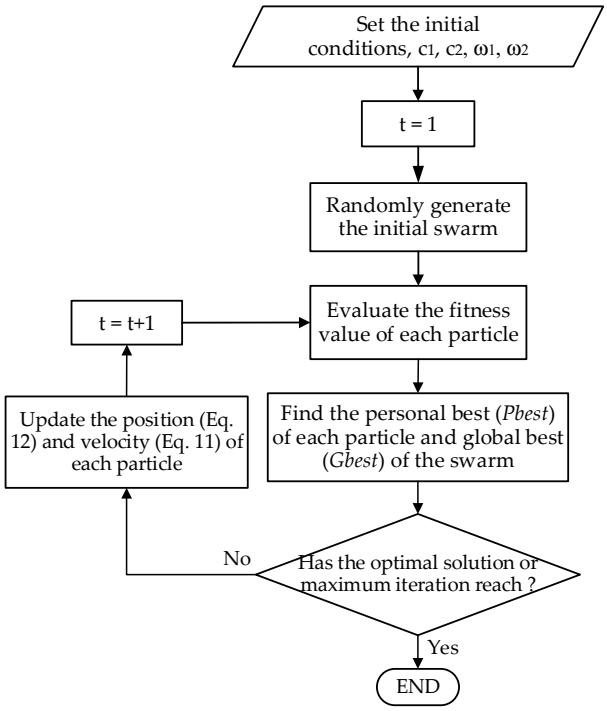

Figure 2. Flow chart of the PSO algorithm.

The HPSO algorithm was proposed by Kang et al. in 2010 [33], and it incorporates the concepts of inertia weight (ω) proposed by Shi et al. [96] and constriction factor (K) proposed by Clerc [97]. Kang et al. [33] proposed the restriction of the comparison of the fitness value to the top 30% of the best particles and keep them, and the remaining particles are crossed-over and selected using a similar approach as the GA to prevent the particles from being trapped in the local optimal region and to improve the convergence and diversity of the original PSO. The three improvements of the HPSO to the original PSO method are:

(1) The use of the linear inertia weight (ω) proposed by Shi et al., that is, multiply the original velocity by an inertia weight to linearly change the original velocity to increase the search ability of particles. This increases the versatility of PSO in the search and is closer to the optimal solution. The improved velocity formula is:

$$v_i^{t+1} = \omega\,(t) \times v_i^t + c_1 \times rand(\,) \times (P_i^t - x_i^t) + c_2 \times Rand(\,) \times \left(P_g^t - x_i^t\right) \tag{13}$$

$$\omega\,(t) = (\omega_1 - \omega_2) \times \frac{(N_t - t)}{N_t} + \omega_2 \tag{14}$$

where,ω_1, ω_2 are the initial and final inertia weight, respectively, and N_t is the total number of iterations.

(2) The use of a constriction factor (K) to improve the PSO algorithm. This can effectively control the stability and trajectory of the particle search process without limiting the maximum speed of the particle movement. The updated formula for the new velocity of an individual in the HPSO method combines the merits of the methods proposed by Shi et al. [96] and Clerc [97], and can be expressed as follows:

$$v_i^{t+1} = K\left\{ \omega\ (t) \times v_i^t + c_1 \times rand(\ ) \times (P_i^t - x_i^t) + c_2 \times Rand(\ ) \times (P_g^t - x_i^t) \right\} \quad (15)$$

$$K = \frac{2}{\left|2 - \varphi - \sqrt{\varphi^2 - 4\varphi}\right|} \varphi = c_1 + c_2,\ \varphi \geq 4 \quad (16)$$

(3) The crossover of the two modified operations of GA and the incorporation of the top 30% selection rule into the algorithm.

The starting population is a set of design variables whose values are randomly generated within a searching space. Each individual (chromosome) of the population is a possible solution to the problem and is formed by parameters (genes) that set the design variables of the problem. All genes are grouped within a vector that represents a chromosome. The swarm of the population is evaluated using the fitness function to determine the personal and global best values of the entire swarm. Subsequently, the top 30% selection is used to sift through the chromosomes with better fitness from the swarm, while the remaining 70% of particles are put into the modified crossover process to increase the diversity of the population and to prevent the particles from being trapped in the local optimal region. The modified crossover process consists of two approaches. First, a random single point is selected to cut the chromosome into two parts. A uniform crossover method is performed on the first half, in which the parents equally contribute each of their gene values to the offspring chromosomes. This enables the mixing of the parent chromosomes at the gene level rather than the segment level. A normal crossover method is performed on the second half, in which the gene values of two parent chromosomes are interchanged at the crossover point. The details of the modified crossover operator are illustrated in Figure 3, in which P_1, P_2 refer to the parent chromosomes and C_1, C_2 indicate the generated children (offspring) chromosomes. After the recombination process during the modified crossover, the fitness values of the parent and offspring chromosomes are calculated for re-evaluations. These chromosomes with fitness values will undergo a top 50% selection again to obtain improved solutions, and the positions and velocities will be updated using a modified standard PSO with inertial weight to determine the "*Pbest*" and "*Gbest*" solutions. The selection rule for new generation particles is depicted in Figure 4. The detailed flow chart of the HPSO algorithm is shown in Figure 5.

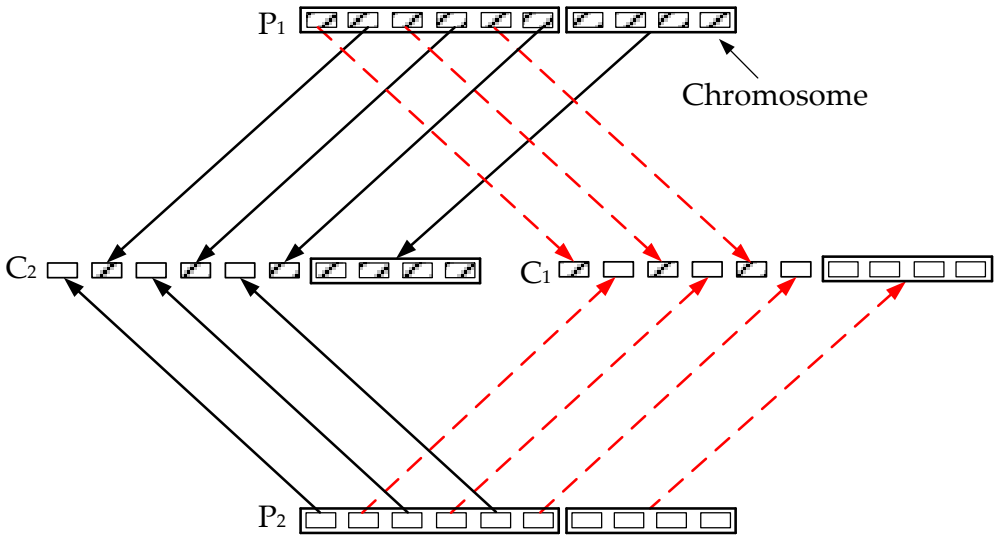

Figure 3. Modified crossover method.

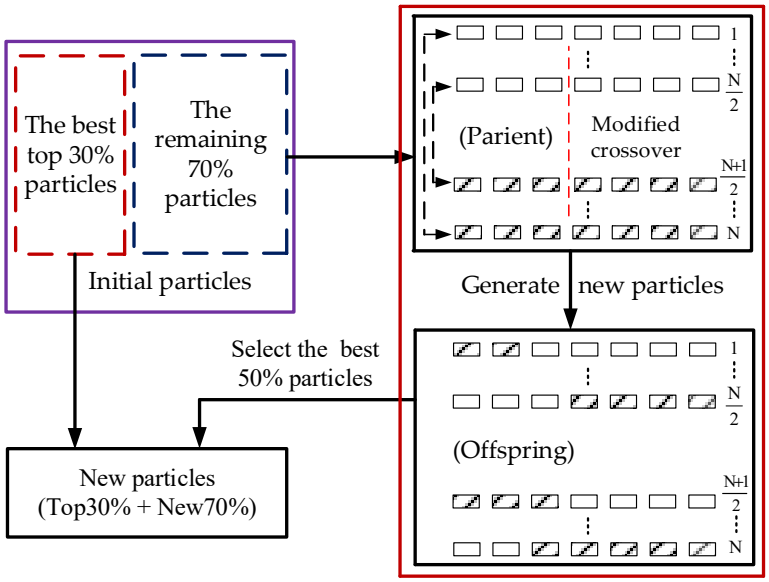

Figure 4. Selection rule of new particles in the hybrid particle swarm optimization (HPSO) method.

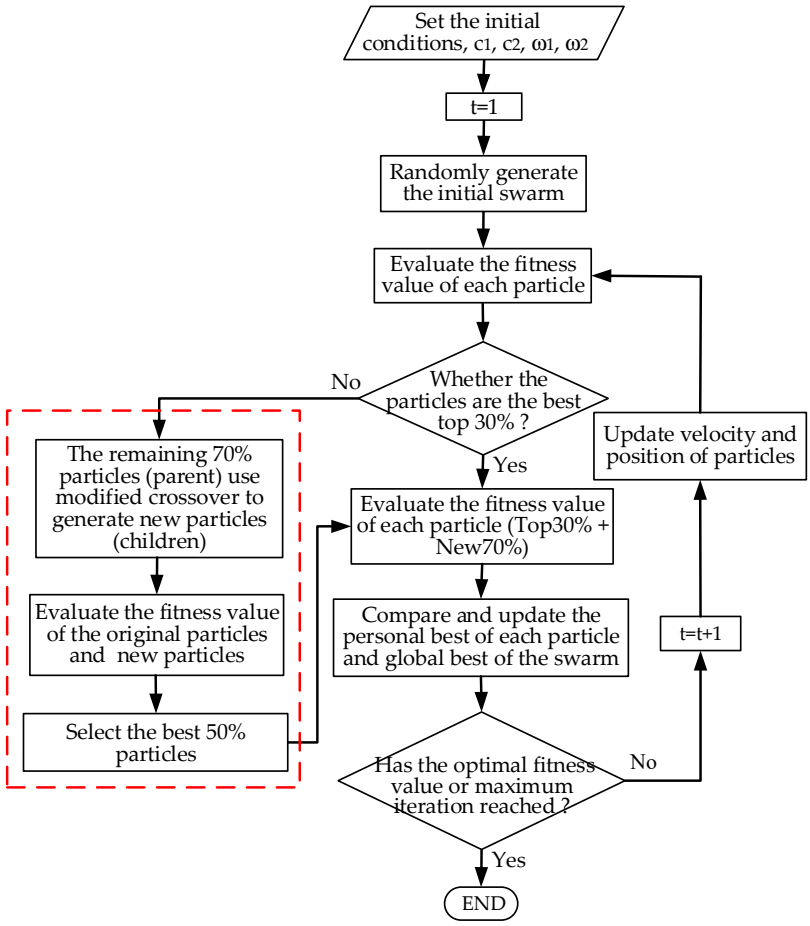

Figure 5. Flow chart of the HPSO algorithm.

3.2. Differential Evolution Algorithm

The differential evolution (DE) algorithm was proposed by Storn and Price in 1997 [30], and it exhibits similar operation mechanism to GA, such as crossover, selection, and muta-

tion. It differs from GA in the first mutation operation, and the concept of difference vector is used in it to make the particles influence each other during movement. The DE algorithm exhibits a high degree of stability and a stronger search ability than PSO and GA. In a D-dimension real variable space, each vector, which is known as a genome/chromosome, forms a potential solution for the optimization problem. The *i*-th parameter vector of the population at the current iteration (*t*) can be denoted using:

$$\mathbf{X}_i{}^t = [x_{i,1}^t,\ x_{i,2}^t, \ldots\ldots,\ x_{i,D}^t] \tag{17}$$

The initial populations (t = 1) should cover the entire parameter space as much as possible by uniformly randomizing distribution within the range constrained by the prescribed minimum and maximum bounds. $\mathbf{X}_{min} = [x_{min,\,1},\ x_{min,\,2},\ \ldots\ ,\ x_{min,\,D}]$ and $\mathbf{X}_{max} = [x_{max,\,1},\ x_{max,\,2},\ \ldots\ ,\ x_{max,\,D}]$ Hence, the *j*-th component of the *i*-th vector can be initialized as

$$x_{i,j}^1 = x_{min,j} + rand_{i,j}(0,\ 1)\ (\ x_{max,j} - x_{min,j}\ )\ (\ i\ =\ 1,\ 2,\ \ldots\ ,\ N_{\mathrm{p}};\ j\ =\ 1,\ 2,\ \ldots\ ,\ \mathrm{D}\ ) \tag{18}$$

where $rand_{i,j}(0,\ 1)$ is a uniformly distributed random number within the interval [0, 1], N_{p} is the number of populations, *i* is the index of the solution vector, and *j* is the index of parameter in vector.

3.2.1. Mutation

After initialization, a mutant vector corresponding to each target vector (parent) $\mathbf{X}_i{}^t$ in the current generation (*t*) is obtained according to the mutation operation. Numerous scholars have proposed different mutation operation methods. The six most widely used mutation strategies are described below:

DE/rand/1:

$$V_i^t = X_{r_1}^t + F(X_{r_2}^t - X_{r_3}^t) \tag{19}$$

DE/best/1:

$$V_i^t = X_{best}^t + F(X_{r_1}^t - X_{r_2}^t) \tag{20}$$

DE/rand/2:

$$V_i^t = X_{r_1}^t + F(X_{r_2}^t - X_{r_3}^t) + F(X_{r_4}^t - X_{r_5}^t) \tag{21}$$

DE/best/2:

$$V_i^t = X_{best}^t + F(X_{r_1}^t - X_{r_2}^t) + F(X_{r_3}^t - X_{r_4}^t) \tag{22}$$

DE/rand-to-best/1:

$$V_i^t = X_i^t + K(X_{best}^t - X_i^t) + F(X_{r_1}^t - X_{r_2}^t) \tag{23}$$

DE/current-to-rand/1:

$$V_i^t = X_i^t + K(X_{r_1}^t - X_i^t) + F(X_{r_2}^t - X_{r_3}^t) \tag{24}$$

where *i* represents an individual in the population, the indices r_1, r_2, r_3, r_4 and r_5 are mutually exclusive integers randomly generated within the range [1, *N*p] and $r_1 \neq r_2 \neq r_3 \neq r_4 \neq r_5 \neq r_i$. $\mathbf{X}_{best}^t$ is the best individual vector with the best fitness function in the population at generation *t*. $\mathbf{X}_{r1} - \mathbf{X}_{r2}$ is the difference vector, *K* is randomly selected within the range [0, 1], and the mutation factor (scale factor) *F* is a positive control parameter for scaling the difference vector and is generally selected within [0.4, 0.99].

3.2.2. Crossover

After the mutation, crossover operation is applied to each pair of the target vector $\mathbf{X}_i{}^t$ and its corresponding mutant vector $\mathrm{V}_i{}^t$ to generate a trial vector (offspring) $\mathbf{U}_i{}^t$ = $[\mathrm{u}^{\mathrm{t}}{}_{\mathrm{i,1}}, \mathrm{u}^{\mathrm{t}}{}_{\mathrm{i,2}}, \ldots\ , \mathrm{u}^{\mathrm{t}}{}_{\mathrm{i,D}}]$. Common crossover methods include single, multi-point crossover,

exponential crossover, and uniform crossover. Uniform (binomial) crossover is generally used, and the formula is as follows:

$$u_{i,j}^{t} = \begin{cases} V_{i,j}^{t} & \text{if } rand_{i,j}(0,\ 1) \le C_r \text{ or } j = j_{rand} \\ x_{i,j}^{t} & \text{otherwise,} \end{cases} \quad j = 1,\ 2,\ \ldots,\ D \tag{25}$$

where j represents the dimension corresponding to the individual, Cr is the user-specified crossover rate within the range [0, 1], $\mathbf{U}_i{}^t$ is the trial vector generated after crossover, and $rand_{i,j}(0,1)$ is a uniform random number in [0, 1] and ensures that the trail vector U_i^t obtains at least one component from the mutant vector $\mathbf{V}_i{}^t$.

3.2.3. Selection

Selection operation determines whether the target vector or trial vector survives the next generation by comparing the corresponding objective function value (fitness value), retaining the better one. If the trial vector exhibits a better fitness value than the target vector, the trial vector will replace the target vector and enter the next generation. Otherwise, the target vector will be retained in the next generation. The selection method often used in the DE algorithm is the competition method, which can be expressed as follows:

$$\mathbf{X}_i^{t+1} = \begin{cases} \mathbf{U}_i^t & \text{if } f(\mathbf{U}_i^t) \le f(\mathbf{X}_i^t) \\ \mathbf{X}_i^t & \text{otherwise} \end{cases} \tag{26}$$

where $\mathbf{X}_i^{t+1}$ is the vector retained to the next generation, $\mathbf{U}_i^t$ is the trial vector and $\mathbf{X}_i^t$ is the target vector. The aforementioned three operations are repeated generation after generation by continuously leaving better vectors, through generation to generation (iterations) and gradually converging, until a termination criterion (i.e., reaching the maximum iteration number of objective function evaluations) is satisfied. The DE algorithm can rapidly determine the best solution. The flow chart of the DE algorithm is shown in Figure 6.

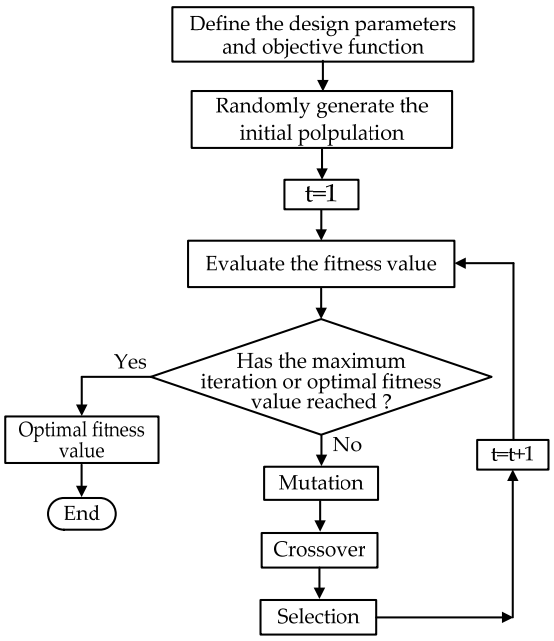

Figure 6. Flow chart of DE algorithm.

3.3. Linearly Ensemble of Parameters and Mutation Strategies in Differential Evolution

The EPSDE method was proposed by Mallipeddi et al. in 2011 [95], and it involves the competition of a pool of mutation strategies with a pool of values corresponding to each associated parameter to produce a successful offspring population. This method selects

three mutation strategies in the DE algorithm to form a pool and enables each individual in an initial population to be randomly assigned a mutation strategy and associated parameter values (mutation and crossover factors) obtained from the respective pools. The mutation strategy and associated parameter values producing a better trial vector (offspring) is retained, with the trial vector emerging as the target vector (parent) in the next generation, whereas those that fail to produce better trial vectors are randomly reinitialized with a new mutation strategy and associated parameter values. The three mutation strategies selected in the EPSDE method to form a pool with diverse characteristics for most optimization problems are as follows:

(1) DE/rand/1
Exhibits stronger exploration capabilities, and it is faster, robust and is one of the most widely used mutation strategies in the DE literature.
(2) DE/best/2
Utilizes two difference vectors, and it is more robust than a strategy that utilizes one difference vector
(3) DE/current-to-rand/1
Takes advantage of its rotation-invariant characteristics, and does not require a crossover operation.

In the EPSDE method, each vector is randomly selected using the aforementioned three mutation methods, thereby utilizing the advantages of the three mutation methods. Mallipeddi et al. [95] suggested that the population size should be kept constant throughout the evolution process, and the value of mutation factor should be taken in the range of [0.4, 0.9] at a step size of 0.1, and the value of the crossover factor should be taken in the range of [0.1, 0.9] at a step size of 0.1. The flow chart of the EPSDE method is shown in Figure 7.

The characteristic feature of the EPSDE method is that the designer does not need to set too many algorithm parameters to adapt to the problem; however, this method exhibits an incomplete convergence and slower speed when dealing with higher dimension problems, resulting in the need to increase the number of groups or iterative number to reach convergence. Tanabe et al. [98] proposed a linear-success-history-based adaptive DE (L-SHADE) method to significantly improve the performance of SHADE using a linear population size reduction (LPSR) method, a simple deterministic population resizing method which continuously reduces the population size according to a linear function, and which only requires the initial population size and population reduction frequency as the user-defined parameters. In addition, it has been experimentally confirmed to exhibit the best overall performance on 30 benchmark problems compared to other DE variants, particularly for higher dimension (D $\in$ [30, 50]) of the optimal design problem.

The LPSR formula for linear population reduction is as follows:

$$N_{t+1} = round\left(N_{init} - \frac{NFE_t}{NFE_{\max}} \cdot (N_{init} - N_{\min})\right) \tag{27}$$

where N_{t+1} is the population size in the next generation, $N_{\min}$ is the minimum number of population size (at the end of the run), N_{init} is the initial number of population size (at t = 1), NFE_t is the current number of fitness evaluations, and $NFE_{\max}$ is the maximum number of fitness evaluations. In the EPSDE method, the population size (Np) is kept constant throughout the evolution process; thus, in this study, based on the benefit of LPSR in L-SHADE, the characteristic of LPSR was incorporated to improve the EPSDE method to linearly reduce the population size during the evolution process to increase the convergence rate to the optimal solution. This improved method was named linearly EPSDE (L-EPSDE), and the flow chart of the L-EPSDE method is shown in Figure 7.

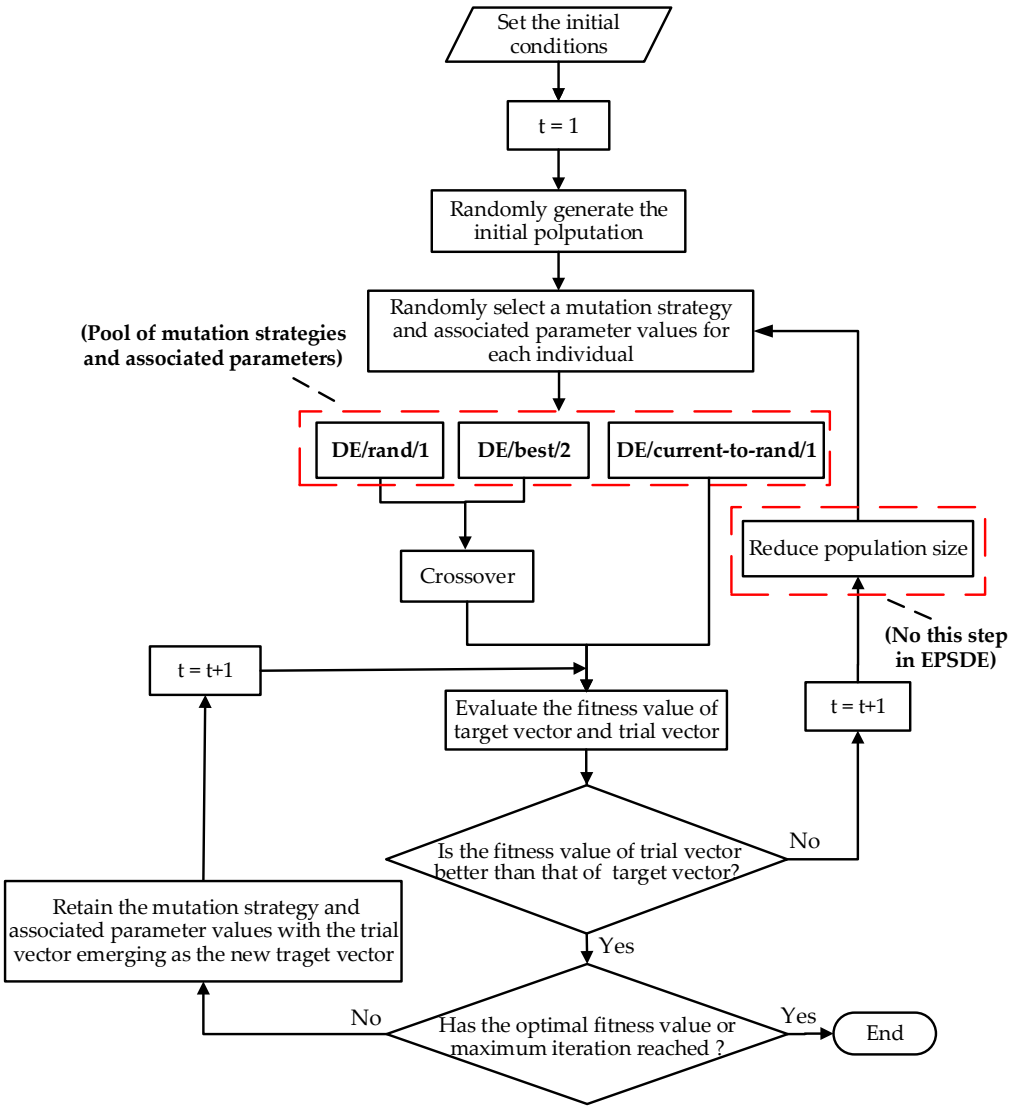

Figure 7. Flow chart of EPSDE and L-EPSDE method.

4. Optimization of Path Generating Four-Bar Linkage

4.1. Objective Function and Constraint Conditions

During the dimensional synthesis of path-generating linkages, the traditional objective function (fitness function) to be minimized is defined as the sum of the squares of the Euclidean distance error between the generated coupler point of the designed four-bar linkage and the desired (target) points. The optimal design involves the determination of the minimum value of the tracing error, which can be expressed as follows:

$$Min \quad f(\mathbf{X}) = \sum_{i=1}^{N_d} \left[\left(C_{xd}^i - C_x^i \right)^2 + \left(C_{yd}^i - C_y^i \right)^2 \right] \tag{28}$$

where $\mathbf{X}$ is the vector of design variables, (C_x^i, C_y^i) is the Cartesian coordinate of the i-th coupler point generated by the designed four-bar linkage, (C_{xd}^i, C_{yd}^i) is the Cartesian coordinate of the i-th desired point, and N_d is the number of desired points.

While designing four-bar linkages, it is essential to consider the restriction relationship of each link so that the motion can meet the requirement. For example, if the desired

four-bar linkage is a crank-rocker mechanism, the constraint formula according to the Grashof's criteria [99] can be expressed as

$$h_1 \ : \ 2[max(r_1, r_2, r_3, r_4) + min(r_1, r_2, r_3, r_4)] < sum(r_1, r_2, r_3, r_4) \tag{29}$$

To prevent the occurrence of order defect (or branch problem), it is necessary to restrict the rotation of the input link in the same order (CW or CCW) during motion. The sequential constraint can be expressed as

$$\begin{array}{c} h_2 \ : \ \theta_2^i > \theta_2^{i+1} > \theta_2^{i+2} > \ldots > \theta_2^{Nd} \\ or \\ h_2 \ : \ \theta_2^i < \theta_2^{i+1} < \theta_2^{i+2} < \ldots < \theta_2^{Nd} \end{array} \tag{30}$$

Once the sequential constraint of the path synthesis problem has been satisfied, the order defect can be avoided. The objective function for the optimal synthesis of a path-generating four-bar linkage is highly constrained and contains two parts. The first part represents the position error between the target points and the generated trajectories of the coupler point of an optimized four-bar linkage, and the second part refers to the restrictions with a penalty function. By adding constraint Equations (29) and (30) to the origin objective function Equation (28), we can obtain:

$$Min \quad f(\mathbf{X}) = \sum_{i=1}^{Nd} \left[\left(C_{xd}^i - C_x^i \right)^2 + \left(C_{yd}^i - C_y^i \right)^2 \right] + M_1 h_1(\mathbf{X}) + M_2 h_2(\mathbf{X}) \tag{31}$$

where $h_{\,1}(\mathbf{X}) = 0$ indicates that the Grashof's condition is true and $h_{\,1}(\mathbf{X}) = 1$ indicates that the Grashof's condition is false; $h_{\,2}(\mathrm{X}) = 0$ indicates that the sequence condition for θ_2 is true and $h_{\,2}(\mathbf{X}) = 1$ indicates that the sequence condition for θ_2 is false. M_1 and M_2 are very large values that penalize the objective function when the constraints fail. Here, those constraints are inserted into the objective function as "penalty terms", and both M_1, M_2 are considered as a large value of 10^6. This is a classical method of handling the constraints of the optimization problem. In this study, the minimization of the objective function subjected to some constraints was investigated for the coupler curves of path-generating four-bar linkages with various numbers of target points.

4.2. Parameters of Optimization Methods

In this study, the aforementioned five metaheuristic global optimization methods were applied to solve five representative dimensional synthesis problems of planar path-generating four-bar linkages, which have been widely investigated in the literature. The five investigated cases include various types of coupler curves, such as non-aligned points curve (Case 1), irregular closed curves (Cases 2), semi-circular arc curves (Case 3), straight-line segment curves (Case 4), and elliptical path curves (Case 5). In Cases 1, 2, and 3, the coupler curves were synthesized with a prescribed timing, indicating that, not only does the sequence of the input angles need to meet the restriction of Equation (30), it also must satisfies some specified angular positions. However, in Cases 4 and 5, the coupler curves were synthesized without prescribed timing.

The parameter settings of the five metaheuristic global optimization methods are shown in Table 1. For each case problem, the number of particle or populations (Np) was 100, the number of maximum iterations ($N_{it\max}$) was 1000 (except in Case 4, where $N_{it\max}$ was 2000), and the number of objective function evaluation (N_F) was $N_F = N_P \times N_{it\max}$. The number of trials performed for each case was 100, and the statistical values (best value, worst value, mean value, median value, and standard deviation (SD)) were evaluated. In each case, the kinematic simulation and the trajectories of the coupler point of the optimal path-generating four-bar linkages obtained using the five metaheuristic optimization methods were executed using the MATLAB 2011R coded program.

The computer used to execute the cases was equipped with Intel(R) Core(TM) i7-4790 CPU @ 3.60 GHz, RAM: 20 GB.

The crossover rate and mutation factor in the conventional DE algorithm are generally assigned randomly or are modified by self-adaptation at each generation. However, in this study, the ratio of the crossover rate to the mutation factor in the DE algorithm was specified as the golden ratio numbers (0.618:0.382), and the fixed values of the crossover rate (0.618) and mutation factor (0.382) lied in and neared the recommended range of [0.1, 0.9] and [0.4, 0.9] [95], respectively. This DE method with specified values of crossover rate (0.618) and mutation factor (0.382) can be called the DE-gr method. To the best of our knowledge, this is the first application of the golden ratio numbers as the crossover rate and mutation factor, and the comparison of the optimal results of the five metaheuristic optimization methods revealed that this special ratio can increase the accuracy and efficiency of the DE-gr method to converge to the optimal solution.

Table 1. Parameters of five optimization methods.

Optimization Method	PSO	HPSO	DE-gr	EPSDE	L-EPSDE
Number of particles or population (N_P)	100	100	100	100	100
Number of iterations (N_{itmax})	1000	1000	1000	1000	1000
Minimum group (NP_{min})	–	–	–	–	5
Crossover method	–	Single point-uniform	Multi-point	Multi-point	Multi-point
Crossover rate (Cr)	–	–	0.618	0.1~0.9	0.1~0.9
Mutation method	–	–	DE/best/1	DE/best/2 DE/rand/1 DE/current-to-rand/1	DE/best/2 DE/rand/1 DE/current-to-rand/1
Mutation factor (F)	–	–	0.382	0.4~0.9	0.4~0.9
Selection method	–	–	Competition law	Competition law	Competition law
Learning factor (c_1, c_2)	2.05	2.05	–	–	–
Inertia weight (ω)	0~1	0~1	–	–	–

4.3. Five Problems of the Dimensional Synthesis of the Path-Generating Four-Bar Linkages

Several previous researchers have investigated these five representative synthesis problems using different algorithms. The comparative study of the results of the metaheuristic optimization methods (DE-gr, PSO, HPSO, EPSDE, and L-EPSDE) employed in this study to those of more than ten other algorithms utilized in previous studies will be discussed in this section. The statistical results (Best, Worst, Median, and Mean values, and SD) of the five metaheuristic methods applied to solve the five selected problems undergoing 100 experimental trials are shown in Table 2. The accuracy and efficiency (effectiveness) of those metaheuristic methods were compared using the SD, mean value, and convergence rate. In Table 2, the bold numbers on each column for all cases are the minimum values of the statistical results of 100 optimal solutions obtained using the five metaheuristic methods.

Table 2. Results of optimized values and statistical analyses of five representative cases.

	Case 1: *5 Target Points, Non-Aligned Point Curve*					**Case 2:** *18 Target Points, Irregular Closed Curve*				
	Best	**Worst**	**Median**	**Mean**	**SD**	**Best**	**Worst**	**Median**	**Mean**	**SD**
PSO	1.16E−05	1.92E−03	4.21E−05	1.12E−04	2.83E−04	1.92E−02	2.53E+00	4.67E−02	2.43E−01	6.33E−01
HPSO	8.01E−06	6.37E−05	4.21E−05	3.95E−05	1.32E−05	1.09E−02	8.43E−01	4.64E−02	1.03E−01	1.50E−01
DE-gr	**7.42E−07**	2.36E−05	7.42E−07	2.36E−06	2.35E−05	1.09E−02	2.53E+00	4.53E−02	2.32E−01	5.93E−01

Table 2. *Cont.*

Case 1: *5 Target Points, Non-Aligned Point Curve*						**Case 2:** *18 Target Points, Irregular Closed Curve*				
	Best	**Worst**	**Median**	**Mean**	**SD**	**Best**	**Worst**	**Median**	**Mean**	**SD**
EPSDE	**7.42E−07**	**7.42E−07**	**7.42E−07**	**7.42E−07**	**9.64E−20**	**9.91E−03**	**2.60E−01**	1.14E−01	1.18E−01	**5.88E−02**
L-EPSDE	**7.42E−07**	**7.42E−07**	**7.42E−07**	**7.42E−07**	1.08E−19	**9.91E−03**	4.53E−01	**4.53E−02**	**7.77E−02**	8.08E−02
Case 3: *6 target points, semi-circular arc curve*						**Case 4:** *6 target points, straight-line segment curve*				
	Best	Worst	Median	Mean	SD	Best	Worst	Median	Mean	SD
PSO	3.26E+00	1.91E+02	7.55E+00	1.21E+01	2.16E+01	5.74E−03	1.68E+01	2.99E+00	4.00E+00	3.38E+00
HPSO	2.95E+00	1.40E+02	8.27E+00	1.55E+01	1.89E+01	4.54E−03	1.43E+01	6.32E+00	6.12E+00	3.09E+00
DE-gr	**2.58E+00**	7.16E+01	4.67E+00	1.02E+01	1.62E+01	**2.32E−04**	2.50E+01	2.36E+00	3.53E+00	4.10E+00
EPSDE	**2.58E+00**	**1.37E+01**	**2.58E+00**	3.47E+00	**1.90E+00**	2.59E−04	8.84E+00	**1.00E−01**	1.17E+00	2.43E+00
L-EPSDE	**2.58E+00**	7.16E+01	**2.58E+00**	**2.91E+00**	5.26E+00	4.71E−04	**7.12E+00**	1.09E−01	**3.24E−01**	**8.15E−01**
						Case 5: *10 target points, elliptical path curve*				
						Best	Worst	Median	Mean	SD
					PSO	2.30E−01	3.44E+02	9.59E+01	1.21E+02	9.81E+01
					HPSO	**5.42E−03**	2.92E+02	1.71E+01	4.96E+02	7.35E+01
					DE-gr	8.00E−03	3.73E+02	4.37E+01	7.51E+01	8.42E+01
					EPSDE	1.83E−02	2.77E+02	4.15E+01	6.47E+01	7.13E+01
					L-EPSDE	7.02E−03	**1.89E+02**	**5.44E+00**	**1.31E+01**	**1.85E+01**

Case 1: Five non-aligned points (5 target points, 6 design variables).

This is a path generation problem with prescribed timing, whose coupler point must trace a path with five non-aligned points. This problem was originally proposed by Kunjur and Krishnamarty [39]. The four-bar mechanism exhibits a crank-fixed point in the coordinate system, and the direction of fixed link is collinear to the *X*-axis, that is $\theta_0 = 0$, $x_0 = 0$, $y_0 = 0$. The problem can be defined as follows:

The coordinates of five target points:

$$\left\{C_d^i\right\} = \{(3.000,\ 3.000)\ ,\ (2.759,\ 3.363)\ ,\ (2.372,\ \ 3.663)\ ,(1.890,\ 3.862)\ ,\ (1.355,\ 3.943)\}$$

The input crank positions for prescribed timing:

$$\left\{\theta_2^i\right\} = \{\pi/6,\ \pi/4,\ \pi/3,\ 5\pi/12,\ \pi/2\}\ (i = 1,\ 2,..,\ 5)$$

The vector of six design variables:

$$\mathbf{X} = [r_1,\ r_2,\ r_3,\ r_4,\ r_{cx},\ r_{cy}]$$

The limits of the design variables:

$$r_1,\ r_2,\ r_3,\ r_4\ \in\ [1/20,\ 12],\ \ r_{cx},\ r_{cy}\ \in\ [-15,\ 15].$$

The synthesized optimal parameters and the corresponding values of the objective function for each method are listed in Table 3. In this work, the design domain was medium-sized with five target points. It is important to note that there was a slight difference in the limits of design variables in previous literature, such as GA-CSP [41] and IOA$^{S\text{-}at}$ [53] methods, $r_1,\ r_2,\ r_3,\ r_4\ \in\ [0,\ 50]$, MUMSA [48] and HLIDE [66] methods, $r_1,\ r_2,\ r_3,\ r_4\ \in\ [0,\ 5], r_{cx},\ r_{cy}\ \in\ [-5,\ 5]$.

Table 3. Optimal results of EPSDE, L-EPSDE, and ten other optimization methods for Case 1.

	GA-KK [39]	Exact Grad. [41]	GA-CSP [41]	MUMSA [48]	$IOA^{S\text{-}at}$ [53]	HLIDE [66]	BAS [37]	ODSRA + CP [75]	REA [76]	HCDJ [77]	EPSDE This Work	L-EPSDE This Work
Np	100	–	50	50	25	100	–	50	–	50	100	100
N_F	5000	39	5000	5000	5000	3900	10,000	5000	3900	5000	100,000	100,000
r_1 (mm)	3.50964	2.85813	3.06304	3.77327	2.80361	3.670110	3.713526	3.6537	1.996566	4.293081	3.66973	3.66973
r_2 (mm)	1.85791	1.99965	1.99596	2.00000	1.99226	1.99781	1.997874	1.9977	3.901976	1.997832	1.99781	1.99781
r_3 (mm)	4.72584	3.06518	3.30582	4.11697	3.30461	3.99675	4.046953	3.9780	2.679281	4.73741	3.99632	3.99632
r_4 (mm)	3.51872	2.46329	2.52471	2.74616	2.47412	2.70500	2.719239	2.7000	1.669044	2.94173	2.70489	2.70489
r_{cx} (mm)	1.95754	1.71710	1.64516	1.67849	1.64413	1.67206	1.67414	1.6677	1.684562	1.70741	1.67205	1.67205
r_{cy} (mm)	1.55890	1.63089	1.70896	1.67098	1.71454	1.68011	1.67796	1.6844	0.0000009	1.64417	1.68013	1.68013
Error	9.54E−04	6.80E−05	1.83E−06	1.77E−06	4.27E−06	**7.42E−07**	**7.467E−07**	7.67E−07	8.64E−07	1.924E−06	**7.42E−07**	**7.42E−07**

The comparison of the optimal solutions of EPSDE and L-EPSDE for Case 1 to those of the three other metaheuristic optimization algorithms and ten other methods are shown in Tables 2 and 3, respectively. The comparison results revealed that the optimal value (7.42E−07) of L-EPSDE was the same as those of the EPSDE and DE-gr (Table 2) and HLIDE methods (Table 3), slightly superior to those of the BAS, ODSRA + CP, and REA methods (Table 3), and superior to those of the PSO, HPSO (Table 2) and GA-KK, Exact gradient, GA-CSP, MUMSA, $IOA^{S\text{-}at}$, and HCDJ methods (Table 3). However, based on the SD and mean value in Table 2, both the L-EPSDE and EPSDE were superior to DE-gr. The trajectories of the coupler point obtained by the five metaheuristic algorithms in Case 1, simulated by a MATLAB coded program, are shown in Figure 8, in which the curves of HPSO, EPSDE, and L-EPSDE coincide with one another, as their optimal solutions were the same. The trajectory of the coupler point and the optimal mechanism obtained by L-EPSDE method are shown in Figure 9. The convergence rates of the five metaheuristic methods are shown in Figure 10. The HPSO method exhibited the best convergence rate to the optimal solution and almost achieved an optimal fitness value at the eleventh generation, and the convergence rate of L-EPSDE was slightly slower than PSO, HPSO, EPSDE, and DE-gr. However, all five metaheuristic optimization methods converged rapidly (under 20 iterations) because the number of design variables was six, which is easier than four other cases.

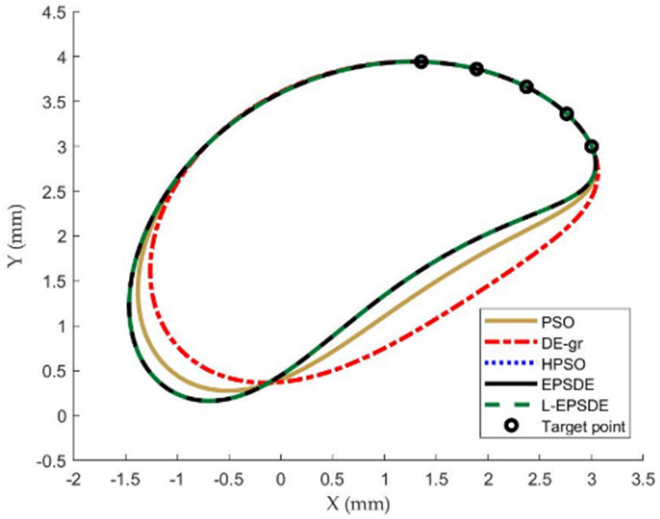

Figure 8. Trajectories of the coupler point of Case 1.

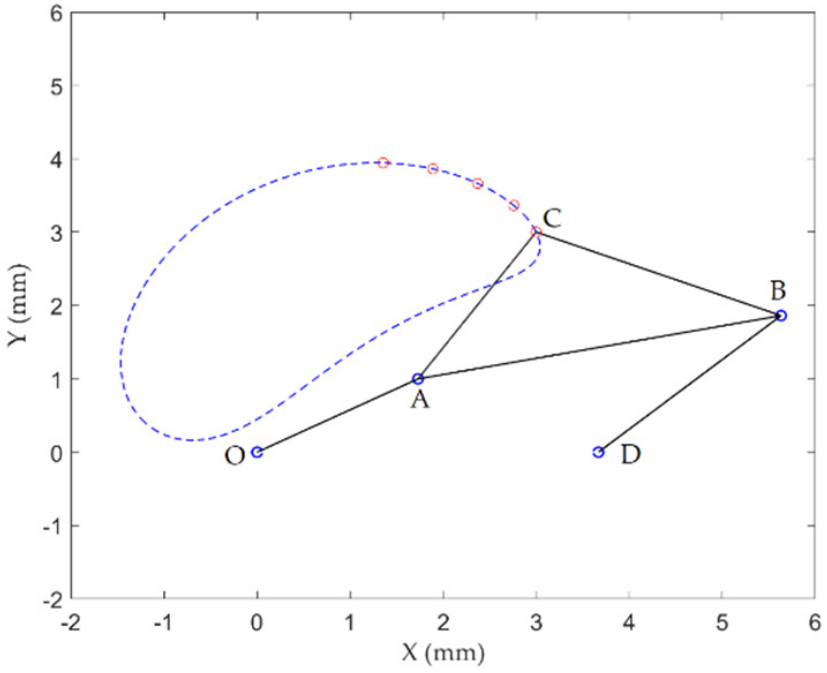

Figure 9. Trajectory of the coupler point of Case 1.

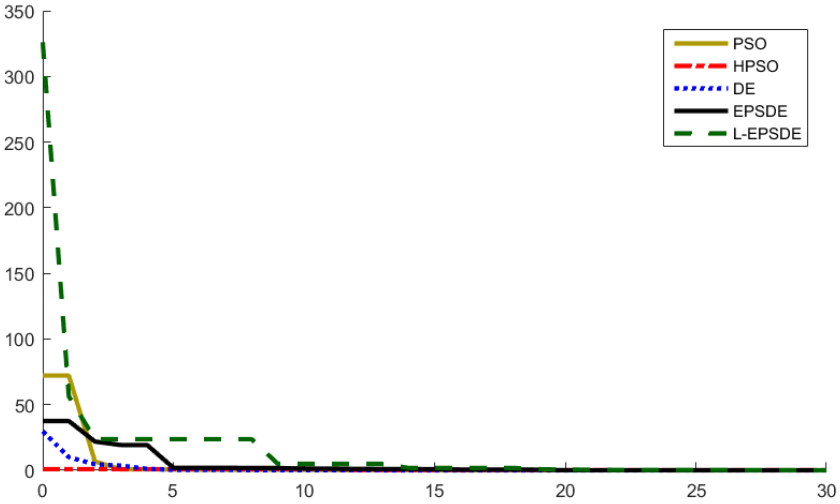

Figure 10. Convergence rate of the five metaheuristic methods for Case 1.

Case 2: Irregular closed curve (18 target points, 10 design variables).

This is a representative problem for the synthesis of path generation with prescribed timing, where 18 target points are specified in an irregular closed curve. This well-known problem was originally proposed by Kunjur and Krishnamarty [39], and has been solved by numerous researchers. The problem is defined as follows:

The coordinates of eighteen target points (unit: mm):

$$\{C_d^i\} = \begin{array}{l}\{(0.5,\ 1.1)\ ,\ (0.4,\ 1.1)\ ,\ (0.3,\ 1.1)\ ,(0.2,\ 1.0)\ ,\ (0.1,\ 0.9)\ ,\ (0.05,\ 0.75),(0.02,\ 0.6)\ ,\ (0,\ 0.5)\ ,\ (0,\ 0.4)\ ,\\ (0.03,\ 0.3)\ ,(0.1,\ 0.25),\ (0.15,\ 0.2),(0.2,\ 0.3)\ ,\ (0.3,\ 0.4)\ ,\ (0.4,\ 0.5)\ ,(0.5,\ 0.7)\ ,\ (0.6,\ 0.9)\ ,\ (0.6,\ 1.0)\}\end{array}$$

The first input crank position, θ_2^1, is a design parameter and prescribed timing with:

$$\theta_2^i = \theta_2^1 + \frac{\pi}{9}(i-1),\ i = 1 \text{ to } 18.$$

The vector of ten design variables:

$$\mathbf{X} = \left[r_1, r_2, r_3, r_4, r_{cx}, r_{cy}, x_0, y_0, \theta_0, \theta_2^1\right]$$

The limits of the design variables:

$$r_1, r_2, r_3, r_4 \in [0, 12]; \quad x_0, y_0, r_{cx}, r_{cy} \in [-15, 15], \theta_0, \theta_2^1 \in [0, 2\pi]. \tag{32}$$

In this study, the design domain exhibits a large size with 18 target points. There are slight differences in the limit of design parameters in various studies, such as the GA-CSP [41], GA-DE [47], MUMSA [48], IOA$^{S\text{-}at}$ [53], HCDJ [77] methods, $r_1, r_2, r_3, r_4 \in [0, 50]$; $x_0, y_0, r_{cx}, r_{cy} \in [-50, 50]$, DE-SRT [56] and BAS [37] methods, $r_1, r_2, r_3, r_4 \in [0, 5]$; r_{cx}, r_{cy}, $x_0, y_0 \in [-5, 5]$. Hereafter, in the following cases, the existence of difference in the limits of design variables will not be mentioned again.

The comparison of the optimal solution of L-EPSDE for Case 2 to those of the PSO, HPSO, DE-gr, and EPSDE algorithms and twenty-two other methods are shown in Tables 2 and 4a,b, respectively. The comparison results revealed that the optimal value (9.91E−03) of L-EPSDE was nearly the same as those of the EPSDE (Table 2), DE-SRT, and MKH methods (Table 4a), the CMDE, CS, BAS, and ODSRA + CP methods (Table 4b), but superior to those of the DE-gr, PSO, HPSO methods (Table 2) and the GA-KK, Exact gradient, GA-CSP, Tabu-gradient, Ant-gradient, GA-FC, GA-DE, MUMSA, IOA$^{S\text{-}at}$ (Table 4a), DE (with reduced design parameters number), ADELI, multi-start, Stackelberg game theory, Anal-FS, and HCDJ methods (Table 4b), and was also superior to those of the TLBO and ATLBO-DA methods (Bureerat et al. [73]). However, the optimal value (9.91E−03) of L-EPSDE was slightly inferior to the optimal value (4.6E−03) of GSA [71]. The obtained optimal parameters of L-EPSDE in this work and ODSRA + CP [75] exhibited nearly the same global minimum solution; however, the efficiency of the L-EPSDE method was higher than those of ODSRA + CP, CS, and CMDE methods, as the utilized population size of L-EPSDE was 100, whereas those of the ODSRA + CP, CS, and CMDE methods were 400, 200, and 200, respectively. Furthermore, both the optimal solutions of GA-DE [54] and ADELI [67] methods were not really optimal solutions, as the length ratio r_{max}/r_{min} reached an unreasonable value of 194 and 192, respectively. The trajectories of the coupler point obtained by the five metaheuristic algorithms in Case 2 are shown in Figure 11, in which the curves of EPSDE and L-EPSDE coincide each other, as their optimal solutions were the same. The trajectory of the coupler point and the optimal mechanism obtained by the L-EPSDE method are shown in Figure 12. The convergence rates of the five metaheuristic methods are shown in Figure 13, in which the convergence rate of L-EPSDE was slightly faster than that of EPSDE, but slower than those of PSO, HPSO, and DE-gr.

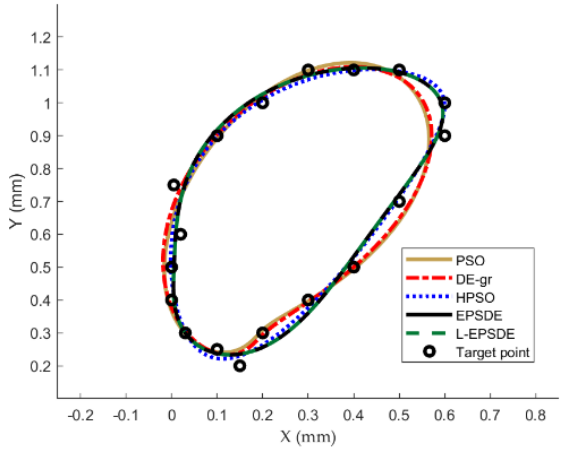

Figure 11. Trajectories of the coupler point of Case 2.

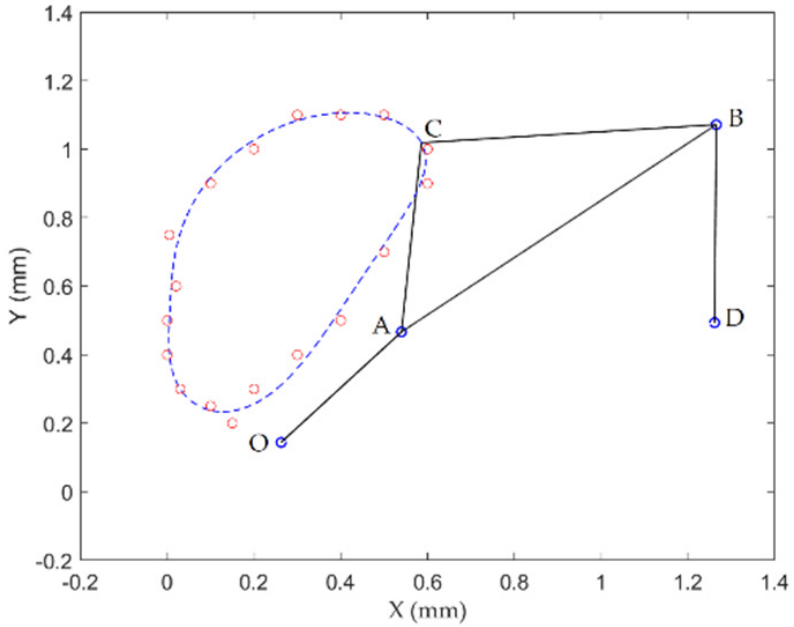

Figure 12. Trajectory of the coupler point of Case 2.

Table 4. (**a**,**b**) Optimal results of L-EPSDE and twenty-two other optimization methods for Case 2.

(a)

	GA-KK [39]	Exact Grad. [41]	GA-CSP [41]	Tabu-Grad. [21]	Ant-Grad. [22]	GA-FC [83]	GA-DE [54]	MUMSA [48]	IOA$^{S\text{-}at}$ [53]	DE-SRT [56]	MKH [34]	L-EPSDE This Work
N_P	100	–	100	–	–	100	100	50	50	200	–	100
N_F	5000	240	5000	550	479	20,000	5000	5000	5000	200,000	25,000	100,000
r_1 (mm)	1.87966	2.85452	3.05788	10.2629	4.1928	1.01	49.9592	4.45377	4.0404	1.05393	1.00429	1.05875
r_2 (mm)	0.27485	0.36355	0.23780	0.3297	0.3333	0.28	0.21861	0.29706	0.2452	0.42388	0.4218	0.42557
r_3 (mm)	1.18025	2.91374	4.82895	0.5012	0.5202	0.36	42.4842	3.91301	6.3829	0.91425	0.87821	0.94469
r_4 (mm)	2.13821	0.49374	2.05646	10.191	4.0224	0.98	32.7470	0.84937	2.6205	0.59892	0.58013	0.57794
r_{cx} (mm)	−0.83359	1.03122	0.76704	0.100	−0.2183	−0.1407	−47.9660	−2.06734	1.1391	0.37060	0.35907	0.38873
r_{cy} (mm)	−0.37877	1.71747	1.85083	0.3805	−0.3040	−0.3314	15.3586	1.66106	1.8661	0.39934	0.38081	0.39467
x_0 (mm)	1.13206	0.95928	1.77681	0.5856	0.5616	0.074	44.1750	−1.30924	1.8918	0.26765	0.26886	0.26244
y_0 (mm)	0.66343	−1.19645	−0.64199	0.7346	0.7409	0.191	−23.9643	2.80696	−0.7613	0.15465	0.17715	0.14396
θ_0 (rad.)	4.35422	0.76398	1.00217	2.9719	−2.9283	−2.4433	5.37543	2.73874	1.1877	0.28482	0.29249	0.33656
θ_2^1 (rad.)	2.55863	0.51172	0.22619	−2.4483	3.4519	–	1.88551	4.85354	0.0000	0.8916	0.88595	0.83767
Error	4.30E−02	1.68E−02	3.37E−02	1.37E−02	1.09E−02	3.78E−02	4.61E−02	1.96E−02	3.49E−02	**9.03E−03**	**9.11E−03**	**9.91E−03**

(b)

	CMDE [60]	CS [35]	DE [63]	ADELI [67]	Multi-Start [65]	Game [93]	BAS [37]	Anal-FC [92]	GSA [71]	ODSRA + CP [75]	HCDJ [77]	L-EPSDE This Work
N_P	200	200	50	–	–	–	40	–	–	400	50	100
N_F	2000,000	400,001	500,000	–	–	–	200,000	–	100,000	400,000	5000	100,000
r_1 (mm)	1.05395	1.05394	1.5395	1.15326	1.400063	11.968126	1.054180	1.1309	0.9695	1.0587	49.80089	1.05875
r_2 (mm)	0.42387	0.42388	0.4102	0.23181	0.402133	0.478725	0.423871	0.4326	0.4246	0.42567	0.28817	0.42557
r_3 (mm)	0.91425	0.91425	1.2166	44.54400	1.362497	8.469510	0.914564	0.9709	0.8209	0.9447	48.47614	0.94469
r_4 (mm)	0.59890	0.59892	1.1230	44.55035	0.540046	8.469510	0.598871	0.5934	0.5955	0.5779	1.63364	0.57794
r_{cx} (mm)	0.37060	0.37060	0.5279	0.70441	0.547398	4.432594	0.3707	0.3765	0.3325	0.3887	−23.41281	0.38873
r_{cy} (mm)	0.39935	0.39935	0.5822	1.10756	0.677040	0.762830	0.3995	0.4086	0.3487	0.3947	7.66449	0.39467

Table 4. *Cont.*

	(b)											
	CMDE [60]	**CS [35]**	**DE [63]**	**ADELI [67]**	**Multi-Start [65]**	**Game [93]**	**BAS [37]**	**Anal-FC [92]**	**GSA [71]**	**ODSRA + CP [75]**	**HCDJ [77]**	**L-EPSDE This Work**
x_0 (mm)	0.26766	0.26766	0.3630	1.29094	0.399159	1.833678	0.267700	0.2409	0.2560	0.2624	−14.83615	0.26244
y_0 (mm)	0.15465	0.15465	−0.0874	−0.10367	−0.170030	4.912576	0.154427	0.1429	0.2214	0.1440	20.14022	0.14396
θ_0 (rad.)	0.28483	0.28482	0.1110	6.22254	0.529247	3.402143	0.285040	0.2878	0.2371	0.3366	2.52861	0.33656
θ_2^1 (rad.)	0.89155	0.89156	0.8721	1.189290	–	3.937901	1.176411	0.8622	1.1692	0.8377	5.06442	0.83767
Error	**9.03E−03**	**9.03E−03**	1.86E−02	2.778E−02	8.971E−02	1.21E−02	**9.03E−03**	1.195E−02	**4.6E−03**	**9.91E−03**	1.608E−02	**9.91E−03**

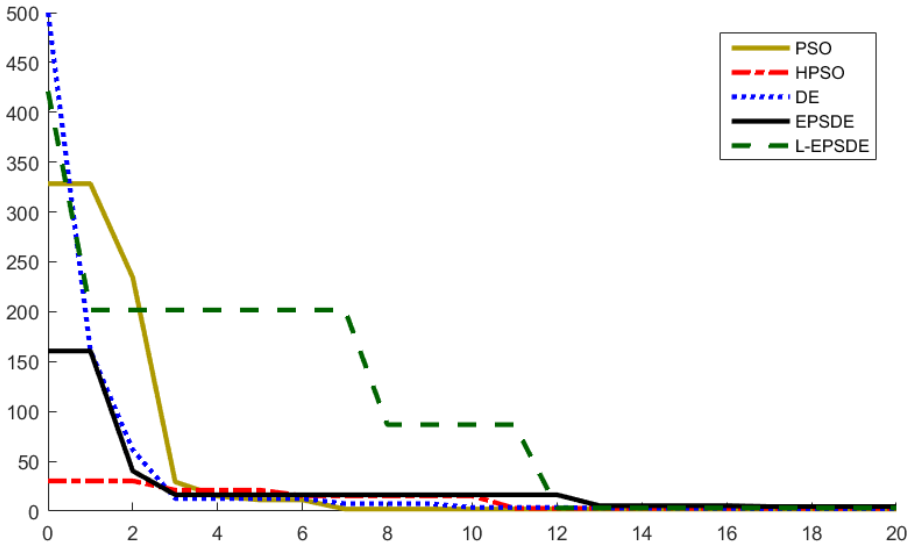

Figure 13. Convergence rate of five metaheuristic methods for Case 2.

Case 3: Semi-circular arc curve (6 target points, 9 design variables).

This is a synthesis problem of path generation with prescribed timing where six target points are specified in a semi-circular curve. This problem was first solved by Acharyya et al. [46] and has been studied by several researchers. The problem can be defined as follows:

The coordinates of six target points:

$$\left\{C_d^i\right\} = \{(0.00,\ 0.00),\ (1.9098,\ 5.8779),\ (6.9098,\ 9.5106),\ (13.09,\ 9.5106),\ (18.09, 5.8779),\ (20.00,\ 0.00)\}$$

The input crank positions for prescribed timing:

$$\left\{\theta_2^i\right\} = \{\pi/6,\ \pi/3,\ \pi/2,\ 2\pi/3,\ 5\pi/6,\ \pi\}\ (i = 1,\ 2, \ldots,\ 6)$$

The vector of nine design variables:

$$\mathbf{X} = \left[r_1, r_2, r_3, r_4, r_{cx}, r_{cy},\ \mathrm{x}_0,\ \mathrm{y}_0,\ \theta_0\right].$$

The limits of the variables:

$$x_0,\ y_0,\ r_{cx},\ \ r_{cy} \in\ [-50,\ 50]; r_1, r_2, r_3, r_4\ \in\ [5,\ 50];\ \theta_0 \in\ [0,\ 2\pi].$$

The comparison of the optimal results of L-EPSDE for Case 3 to those of the PSO, HPSO, DE-gr, and EPSDE methods and eleven other methods are shown in Tables 2 and 5, respectively. It revealed that the optimal value (2.58036) of L-EPSDE was similar to those of the DE-gr and EPSDE methods (Table 2) and MUMSA, HLIDE, and REA methods (Table 5), and superior to those of the PSO and HPSO methods (Table 2), the DE, GA-DE, ICA and

HTRCA methods (Table 5), and inferior to those of the DE (reduced number of design parameters) [63], IOA$^{S\text{-}at}$, BAS, and HCDJ methods (Table 5) and the ATLBO-DA method (Bureerat et al. [73]). The trajectories of the coupler point obtained by five metaheuristic algorithms in Case 3 are shown in Figure 14, in which the curves of DE-gr, EPSDE, and L-EPSDE coincide one another, as their optimal solutions were same. The trajectory of the coupler point and optimal mechanism obtained by the L-EPSDE method is shown in Figure 15. The convergence rates of the five metaheuristic methods are shown in Figure 16, which indicated that the convergence rate of L-EPSDE was faster than those of PSO, EPSDE, and HPSO, but was slightly slower than DE-gr.

Table 5. Optimal results of L-EPSDE and eleven other optimization methods for Case 3.

	DE [46]	GA-DE [47]	MUMSA [48]	IOA$^{S\text{-}at}$ [53]	ICA [55]	HTRCA [91]	DE [63]	HLIDE [66]	BAS [37]	REA [76]	HCDJ [77]	L-EPSDE This Work
Np	100	100	100	50	–	–	80	100	40	–	50	100
N_F	1000	100,000	100,000	100,000	–	–	800,000	50,000	120,000	90, 000	50,000	100,000
r_1 (mm)	50.00000	50.00000	50.00000	49.96897	50.00000	49.46	43.30492	50.00000	47.23450	49.999992	49.999980	50.00000
r_2 (mm)	5.00000	5.00000	5.00000	4.78566	5.00000	5.504	11.1149	5.00000	8.84740	5.000002	1.348432	5.00000
r_3 (mm)	5.90535	6.97009	7.03105	6.49103	7.08248	8.015	42.6226	7.03091	25.04747	7.031010	1.348451	7.03105
r_4 (mm)	50.00000	48.1993	48.13418	48.39394	48.05733	47.165	11.9381	48.13432	50.00000	48.134251	50.000000	48.13418
r_{cx} (mm)	18.81931	17.045	16.97669	16.44478	16.4264	17.9	51.9215	16.9770	42.02840	16.976890	11.384434	16.97669
r_{cy} (mm)	0.00000	12.638	12.95214	11.98809	13.7111	15.3	−7.1475	12.95115	−27.08529	12.952033	4.442436	12.95214
x_0 (mm)	14.37377	12.2377	12.19749	12.04659	11.88034	12.0	−43.3598	12.19769	16.55312	12.197689	10.194752	12.19749
y_0 (mm)	−12.44430	−15.8332	−15.99820	−14.7749	−16.08766	−18.7	−0.0067	−15.9978	−48.14738	−15.99843	−3.694134	−15.9982
θ_0 (rad.)	0.463633	0.05085	0.04282	0.03868	6.28319	6.2832	6.2819	0.04286	0.82260	0.042844	6.215880	0.04282
Error	5.52	**2.58286**	**2.58035**	**2.491**	2.5998	3.571	**2.10037**	**2.58036**	**0.78637**	**2.58036**	**1.216212**	**2.58036**

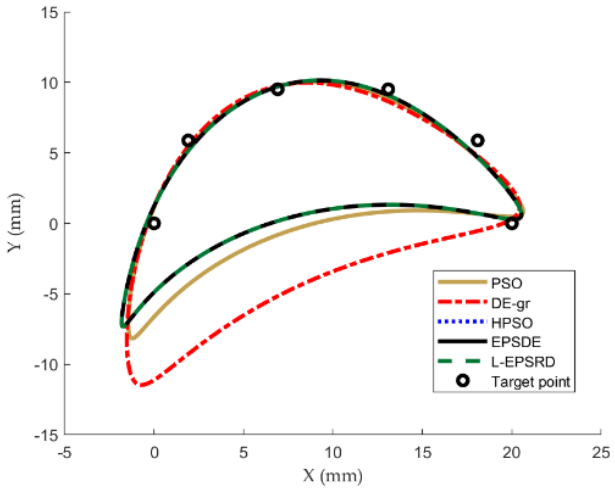

Figure 14. Trajectories of the coupler point of Case 3.

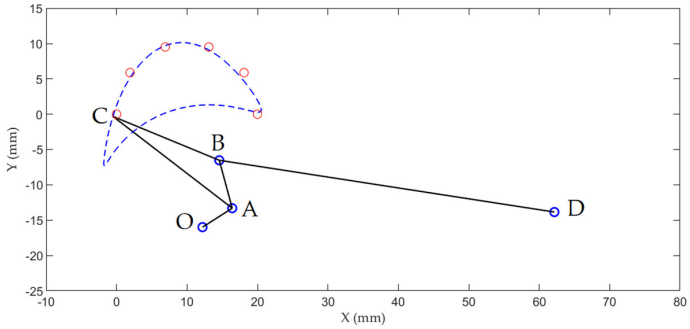

Figure 15. Trajectory of the coupler point of Case 3.

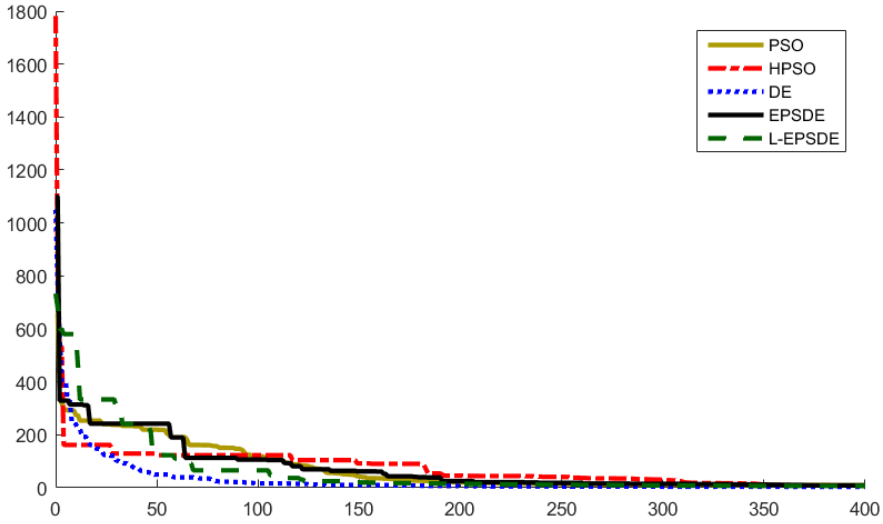

Figure 16. Convergence rate of the five metaheuristic methods for Case 3.

Case 4: Straight-line segment curve (6 target points, 15 design variables)

This is a synthesis problem for the path generation without prescribed timing where six target points are specified in a vertical line segment. This problem was first presented by Cabrera [41] and has been investigated by several researchers. The problem can be defined as follows:

The coordinates of six target coupler points:

$$\left\{C_d^i\right\} = \{(20,\ 20),\ (20,\ 25),\ (20,\ 30),\ (20,\ 35),\ (20,\ 40),\ (20,\ 45)\}$$

The vector of fifteen design variables:

$$\mathbf{X} = \left[r_1, r_2, r_3, r_4, r_{cx}, r_{cy},\ \mathrm{x}_0,\ \mathrm{y}_0,\ \theta_0, \theta_2^1, \theta_2^2, \theta_2^3, \theta_2^4, \theta_2^5, \theta_2^6\right].$$

The limits of the variables:

$$r_1, r_2, r_3, r_4 \in [5,\ 60];\ \ r_{cx},\ r_{cy},\ x_0,\ y_0 \in [-60,\ 60]; \theta_0,\ \theta_2^i (i = 1,\ 2,\ \ldots\ ,6) \in [0,\ 2\pi].$$

The comparison of the optimal synthesis results of the DE-gr and L-EPSDE methods for Case 4 to those of the PSO, HPSO, and EPSDE methods and sixteen other methods are shown in Tables 2 and 6a,b, respectively. The optimal value (4.71E−04) of L-EPSDE was superior to those of the PSO and HPSO methods (Table 2), the GA-CSP, DE, GA-DE, HPSO, ICA, and HTRCA methods (Table 6a), the SAP-TLBO, TLBO, ImHS, GSEF-IAA, and RBDO-MCS methods (Table 6b), and the ATLBO-DA method (Bureerat et al. [73]), but was inferior to those of the MUMSA, IOA$^{\text{S-at}}$, and MKH methods (Table 6a), and the HLIDE, ODSRA + CP, and HCDJ methods (Table 6b). In addition, although the optimal solutions (2.32E−04 and 2.59E−04) of both the DE-gr and EPSDE methods were slightly superior to that of the L-EPSDE method, the mean value (0.324) and SD (0.815) of L-EPSDE were the lowest, indicating that L-EPSDE exhibited the best accuracy and efficiency. The trajectories of the coupler point obtained by the five metaheuristic algorithms in Case 4 are shown in Figure 17, and the trajectory of the coupler point and optimal mechanism obtained by the L-EPSDE method are shown in Figure 18. In this case, the maximum iterative number was 2000. The convergence rates of the five metaheuristic methods are shown in Figure 19, the convergence rate of L-EPSDE was faster than those of HPSO and EPSDE, which converged to an optimal solution of more than 1500 iterations, but slightly slower than those of DE-gr and PSO, which converged to optimal solution less than 100 iterations.

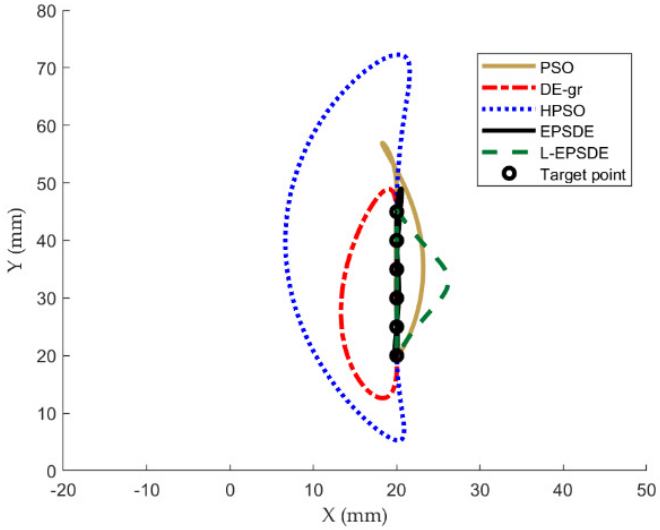

Figure 17. Trajectories of the coupler point of Case 4.

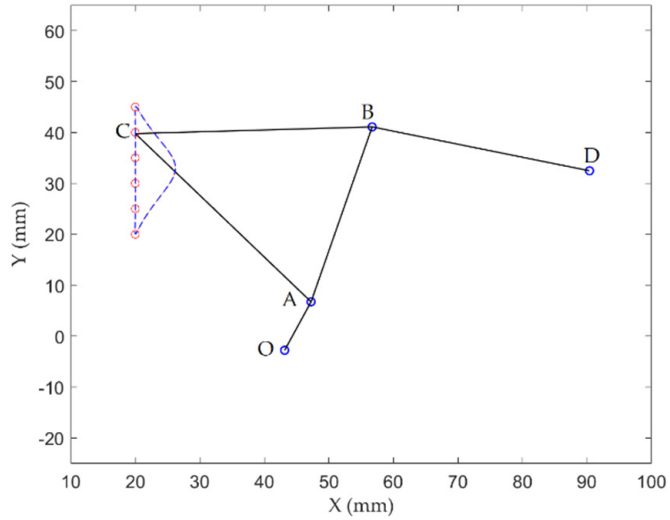

Figure 18. Trajectory of the coupler point of Case 4.

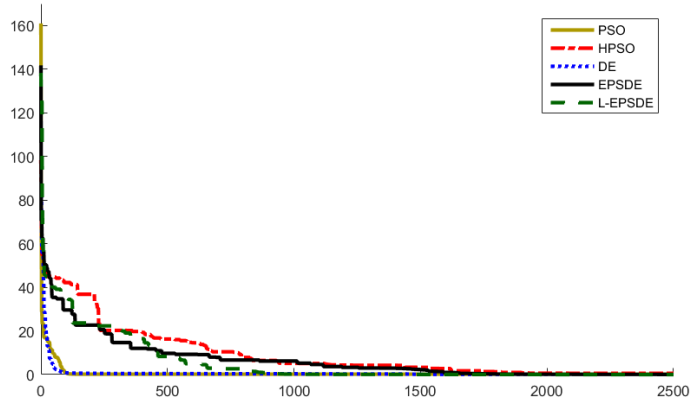

Figure 19. Convergence rate of the five metaheuristic methods for Case 4.

Table 6. (**a**,**b**) Optimal results of DE-gr, L-EPSDE, and sixteen other optimization methods for Case 4.

(a)

	GA-CSP [41]	DE [46]	GA-DE [47]	MUMSA [48]	IOA$^{S\text{-}at}$ [53]	ICA [55]	MKH [34]	HTRCA [91]	DE-gr This Work	L-EPSDE This Work
Np	100	100	100	100	50	–	25	–	100	100
N_F	100,000	100,000	100,000	100,000	100,000	–	25,000	–	200,000	200,000
r_1 (mm)	39.46629	35.02074	33.5959	31.78826	54.71582	60.0000	34.36458	18.42	44.9998	58.94653
r_2 (mm)	8.56291	6.40420	5.02972	8.20465	18.73099	17.51102	7.97728	35.14	16.2478	10.35726
r_3 (mm)	19.09486	31.60722	11.1847	24.93213	31.22310	60.0000	26.95316	56.42	34.5751	35.62035
r_4 (mm)	47.83886	50.59949	28.0878	31.38593	42.22374	33.2268	32.28634	49.99	36.5490	34.77291
r_{cx} (mm)	13.38556	20.80324	−24.1755	34.19372	−27.2984	−28.6280	36.96182	55.08	−1.8620	24.58724
r_{cy} (mm)	12.21961	41.54364	5.51479	14.41567	31.65051	−52.7299	19.66793	−59.52	41.7710	35.03822
x_0 (mm)	29.72255	60.00000	39.7799	−6.36652	43.07086	60.0000	−11.09434	−25.92	45.5386	43.14491
y_0 (mm)	23.45454	18.07791	24.7195	56.83676	27.41706	−1.45505	58.82813	42.12	18.1837	−2.77085
θ_0 (rad.)	6.20163	0.00000	5.45884	4.01596	5.97746	0.93032	4.02771	5.9313	0.1859	0.64073
θ_2^1 (rad.)	6.11937	6.28319	0.524005	1.36655	6.42411	5.54638	1.50348	2.34740	−0.1661	4.93899
θ_2^2 (rad.)	0.19304	0.26494	0.853145	2.33077	6.53496	5.70544	2.38566	2.58490	−0.0325	5.74501
θ_2^3 (rad.)	0.44083	0.50038	1.16505	2.87104	0.36230	5.85061	2.91751	2.84754	0.0933	6.11814
θ_2^4 (rad.)	0.68467	0.73532	1.49253	3.39459	0.46906	5.99041	3.42257	3.11772	0.2174	0.17071
θ_2^5 (rad.)	0.958335	0.99653	1.87456	3.97096	0.57765	6.13185	3.96923	3.37658	0.3449	0.54382
θ_2^6 (rad.)	1.35533	1.33355	2.44206	4.96349	0.69047	6.28318	5.18616	3.61158	0.4812	1.27020
Error	2.62 E−02	1.23E−01	7.37E−04	**2.06E−04**	**2.37E−04**	2.0E−03	**2.37E−05**	5.6E−03	**2.32E−04**	**4.71E−04**

(b)

	SAP-TLBO [58]	TLBO [62]	HLIDE [66]	ImHS [70]	GSEF-IAA[74]	ODSRA + CP [75]	RBDO-MCS [94]	HCDJ [77]	DE-gr This Work	L-EPSDE This Work
Np	100	150	100	–	–	100	–	100	100	100
N_F	–	82,500	100,000	–	25,000	100,000	–	100,000	200,000	200,000
r_1 (mm)	59.9864	60.0000	9.50437	49.334	30.3659	24.7256	55.7371	14.20137	44.9998	58.94653
r_2 (mm)	52.6078	14.6488	5.32006	12.095	10.1183	12.6722	9.3933	8.01431	16.2478	10.35726
r_3 (mm)	56.7209	47.6577	50.79235	35.234	41.018	29.4207	41.8429	16.30992	34.5751	35.62035
r_4 (mm)	59.3396	59.9128	52.45868	38.446	43.0375	34.5590	41.8429	12.25387	36.5490	34.77291
r_{cx} (mm)	53.0988	66.7653	17.28743	26.466	−25.8055	58.6473	42.3130	27.79772	−1.8620	24.58724
r_{cy} (mm)	−56.6734	−63.5825	−31.80356	0.75083	33.9840	0.1583	37.7486	11.30541	41.7710	35.03822
x_0 (mm)	−39.3209	−55.5544	−10.87584	47.33	−12.548	−24.7229	59.1841	−2.30953	45.5386	43.14491
y_0 (mm)	59.9851	1.8752	36.94543	0.5213	29.0686	1.3009	−7.3972	45.69508	18.1837	−2.77085
θ_0 (rad.)	3.6177	4.4871	5.53592	–	–3.4795	1.7411	7.0812	4.51724	0.1859	0.64073
θ_2^1 (rad.)	2.9048	3.5408	1.92725	–	3.43788	2.8192	–	6.25324	−0.1661	4.93899
θ_2^2 (rad.)	2.9995	3.9269	2.50525	–	3.2624	3.1006	–	2.40390	−0.0325	5.74501
θ_2^3 (rad.)	3.0942	4.2133	3.08097	–	3.10181	3.3863	–	2.93624	0.0933	6.11814
θ_2^4 (rad.)	3.1890	4.4653	3.66536	–	2.9464	3.6770	–	3.49056	0.2174	0.17071
θ_2^5 (rad.)	3.2837	4.7052	4.24372	–	2.78698	3.9769	–	4.06508	0.3449	0.54382
θ_2^6 (rad.)	3.3784	4.9469	4.82479	–	2.61095	4.2996	–	5.20950	0.4812	1.27020
Error	8.82E−04	1.48E−01	**5.18E−07**	8.76E−03	7.95E−04	**8.66E−06**	6.0E−04	**8.84E−29**	**2.32E−04**	**4.71E−04**

Case 5: Elliptical path curve (10 target points, 19 design variables)

This is a synthesis problem for path generation without prescribed timing [46]. The ten target points are specified in an elliptical path, whose major and minor axes consisted of 20 and 16 units, respectively, and the center is kept at (10,10). The problem can be defined as follows:

The coordinates of ten target points:

$$\{C_d^i\} = \{\,(20.00, 10.00), (17.66, 15.142), (11.736, 17.878), (5.00, 16.928), (0.60307, 12.736), (0.60307, 7.2638), (5.00, 3.0718), (11.736, 2.1215), (17.66, 4.8577), (20.00, 10.00)\}$$

The vector of nineteen design variables:

$$\mathbf{X} = \left[r_1, r_2, r_3, r_4, r_{cx}, r_{cy}, \mathrm{x}_0, \mathrm{y}_0, \theta_0, \theta_2^1, \theta_2^2, \theta_2^3, \theta_2^4, \theta_2^5, \theta_2^6, \theta_2^7, \theta_2^8, \theta_2^9, \theta_2^{10}\right].$$

The limits of the variables:

$$r_1, r_2, r_3, r_4 \in [5, 80]; \; r_{cx}, r_{cy}, x_0, y_0 \in [-80, 80]; \theta_0, \theta_2^i (i = 1, 2, \ldots, 10) \in [0, 2\pi].$$

The comparison of the optimal synthesis results of the HPSO and L-EPSDE methods for Case 5 to those of the PSO, DE-gr, and EPSDE methods and eleven other methods are shown in Tables 2 and 7, respectively. It revealed that the optimal value (7.02E−03) of L-EPSDE was superior to those of the DE-gr, PSO, and EPSDE methods (Table 2) and the DE, GA-DE, IOA$^{S\text{-}at}$, HTRCA, and GSA methods (Table 7), and that it was also superior to those of the SAP-TLBO (Sleesongsom et al. [58]) and ATLBO-DA methods (Bureerat et al. [73]), but was slightly inferior to those of the HPSO, MUMSA, DE-SRT, CMDE, HLIDE, GSA, and REA methods (Table 7) and the TLBOE method (Zhang et al. [72]). In addition, although the optimal value (5.42E−03) of HPSO was superior to that of L-EPSDE, the mean value (1.31) and SD (1.85) of L-EPSDE (Table 2) were smaller than those of the four other metaheuristic methods, indicating that L-EPSDE exhibited the best accuracy and efficiency. The trajectories of the coupler point obtained by the five metaheuristic algorithms in Case 5 are shown in Figure 20, in which the curves of PSO, HPSO, EPSDE, and L-EPSDE are very close, and the trajectory of the coupler point and optimal mechanism obtained by the L-EPSDE method are shown in Figure 21. The convergence rates of the five metaheuristic methods are shown in Figure 22. The convergence rate of L-EPSDE was closer to that of HPSO compared to that of EPSDE, but slower than those of DE-gr and PSO.

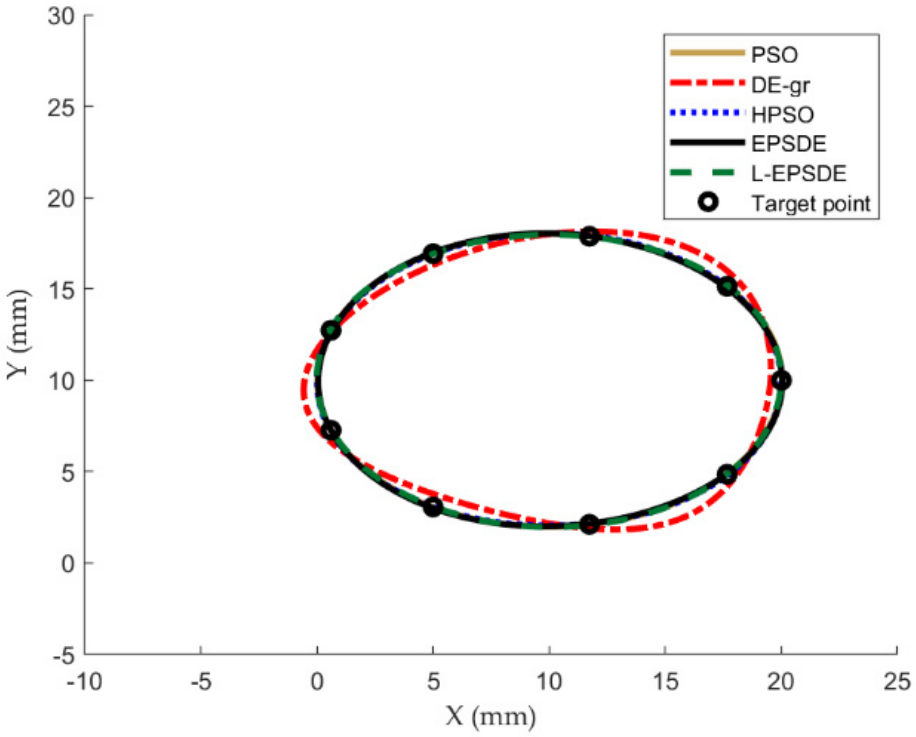

Figure 20. Trajectories of the coupler point of Case 5.

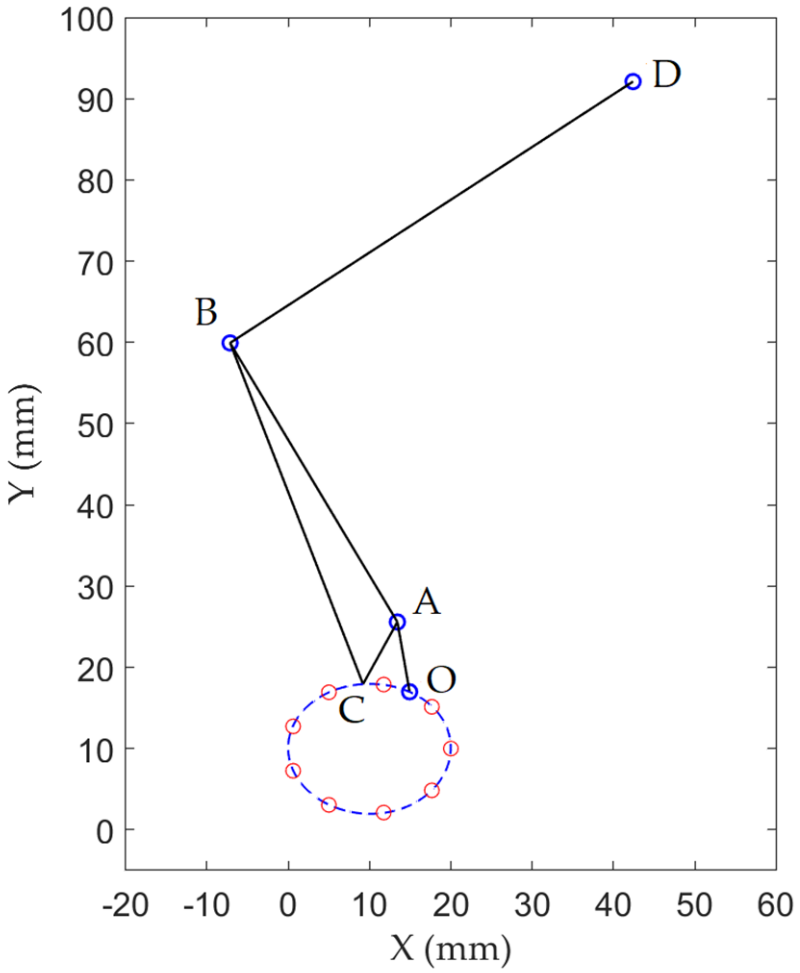

Figure 21. Trajectory of the coupler point of Case 5.

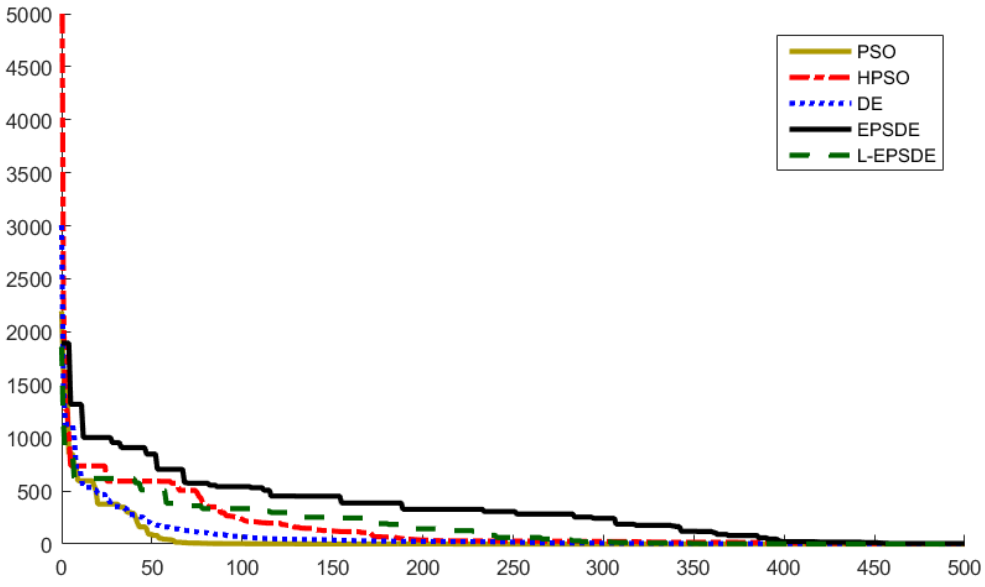

Figure 22. Convergence rate of the five metaheuristic methods for Case 5.

Table 7. The optimal results of HPSO, L-EPSDE, and eleven other optimization methods for Case 5.

	DE [46]	GA-DE [47]	MUMSA [48]	IOA$^{S\text{-}at}$ [53]	DE-SRT [56]	HTRCA [91]	CMDE [60]	TLBO [64]	HLIDE [66]	GSA [71]	REA [76]	HPSO This Work	L-EPSDE This Work
N_P	100	100	100	50	100	–	100	500	50	–	–	100	100
N_F	100,000	100,000	100,000	100,000	100,000	–	100,000	50,000	100,000	100,000	100,000	100,000	100,000
r_1 (mm)	54.36089	80.0000	79.51607	65.42877	79.9985	54.857	80.00000	42.0053	80.00000	63.0882	79.99431	66.14036	79.98736
r_2 (mm)	8.68335	8.24689	9.72397	8.01639	8.72535	9.725	8.04566	8.0876	8.203235	9.5896	8.117863	8.02857	8.72534
r_3 (mm)	34.31863	45.8968	45.84252	47.22166	51.8801	49.925	50.81902	28.2600	52.34788	39.7516	51.10882	37.27658	40.04208
r_4 (mm)	79.99617	58.5404	51.43285	44.13656	43.3619	23.375	42.20801	24.1099	41.17572	34.4096	42.17296	38.55923	59.08385
r_{cx} (mm)	0.00019	−6.40389	8.21392	−11.5709	−6.63658	7.840	−10.6370	−4.4860	−10.9879	6.5766	−10.9301	−6.61025	−4.38869
r_{cy} (mm)	1.46525	−9.12264	−2.95396	−1.90491	8.2734	−4.320	−2.29109	−4.7935	1.97982	2.3035	−0.00687	−3.30141	7.55335
x_0 (mm)	10.95440	6.52409	2.02111	10.63541	15.9712	1.440	8.49481	11.1765	6.74348	3.9094	7.575251	3.68216	14.92300
y_0 (mm)	11.07453	20.5220	13.21659	−1.67548	18.5445	12.160	−0.75797	3.5870	−0.60110	7.0455	−0.61085	9.42430	16.98752
θ_0 (rad.)	2.12965	0.136532	5.59694	3.86733	1.34791	6.1135	3.88921	2.73892	4.12317	0.6061	4.009837	2.63731	1.22009
θ_2^1 (rad.)	6.28319	6.05991	0.63769	2.41993	5.04915	0.14828	2.44944	6.26862	2.24025	0.0480	2.344066	2.65557	5.17437
θ_2^2(rad.)	0.61673	0.488453	1.32553	3.10927	5.73644	0.82561	3.15397	0.66488	2.95502	0.07579	3.054448	3.35029	5.86615
θ_2^3 (rad.)	1.31025	1.17805	2.00803	3.81295	0.13974	1.52053	3.83711	1.33889	3.64900	1.4689	3.742718	4.01064	0.27374
θ_2^4 (rad.)	2.19357	1.88339	2.69557	4.50644	0.832578	2.23681	4.52017	2.01652	4.33396	2.1897	4.426518	4.69612	0.96047
θ_2^5 (rad.)	2.91717	2.59806	3.38458	5.18114	1.53611	2.90660	5.20480	2.70122	5.01670	2.9098	5.109552	5.38508	1.66772
θ_2^6 (rad.)	3.49075	3.28585	4.08294	5.88342	2.24424	3.56508	5.89854	3.42419	5.70450	3.6268	5.799614	6.08002	2.37867
θ_2^7 (rad.)	4.13202	3.96674	4.79845	0.29626	2.96272	4.29519	0.316204	4.13519	0.11548	4.2894	0.214054	0.5060	3.08000
θ_2^8 (rad.)	4.92208	4.65966	5.51171	0.99115	3.66871	5.02152	1.023356	4.84542	0.81571	4.9616	0.917886	1.22339	3.79256
θ_2^9 (rad.)	5.69537	5.35231	6.21279	1.70779	4.36455	5.71896	1.73899	5.57812	1.52796	5.6481	1.631829	1.94338	4.49363
θ_2^{10} (rad.)	6.28297	6.06263	0.63719	2.41887	5.04915	0.14283	2.44944	6.26817	2.24025	0.0481	2.344052	2.65573	5.174236
Error	1.952326	3.12E−02	**4.70E−03**	1.91E−02	**4.56E−04**	1.65E−01	**4.02E−04**	1.92E−02	**5.77E−04**	**2.88E−03**	**4.17E−04**	**5.42E−03**	**7.02E−03**

5. Discussion

The golden ratio numbers (0.618:0.382) were selected as the parameters of the cross rate and mutation factor in the traditional DE method, and this so-called DE-gr method increased the rapid exploitation ability for searching for an optimal solution, as shown in the convergence rate of each case. In addition, all the five metaheuristic optimization methods exhibited a similar convergence trend; however, DE-gr generally converged more rapidly to the optimal solution than other methods. According to the statistical results shown in Table 2, in Cases 1 to 3, which are middle dimensional problems (the numbers of design variables are lower or equal to 10), the EPSDE, and L-EPSDE methods obtained the same optimal values, though EPSDE slightly outperformed DE-gr and L-EPSDE, as it exhibited the smallest SD. Further, DE-gr was superior to PSO and HPSO. However, in Cases 4 and 5, which are high dimensional problems (15 and 19 design variables, respectively), L-EPSDE exhibited smaller optimal solutions and a smaller SD than EPSDE, indicating the slight superiority of the accuracy and efficiency of L-EPSDE than those of EPSDE; however, both of them were superior to DE-gr and PSO. In contrast, HPSO exhibited smaller optimal values and SD than PSO in all five cases, indicating that it exhibited enhanced accuracy and efficiency than PSO; however, in high dimensional problems, it exhibited a more enhanced performance than DE-gr. Moreover, HPSO obtained a more enhanced optimal solution than EPSDE and L-EPSDE in Case 5. A comparative ranking of the five metaheuristic optimization methods for solving the five representative synthesis problems of a path-generating four-bar linkage is shown in Figure 23. For each term in all cases, the score of the first is 5, the second is 4, and it decreased sequentially. The total score is the summation of each term in the five cases. In this study, L-EPSDE exhibited the highest best and worst values, and the mean value and SD of L-EPSDE were higher and lower than those of EPSDE, respectively; however, both the mean value and the SD of EPSDE and L-EPSDE were larger than those of DE, PSO, and HPSO. In addition, the best value of EPSDE, L-EPSDE, and DE-gr were slightly different, but the difference in the mean value of L-EPSDE and EPSDE was larger than that in the SD of L-EPSDE and EPSDE, indicating the enhanced accuracy, efficiency, and stability of L-EPSDE and EPSDE than DE-gr, PSO, and HPSO; however, L-EPSDE was slightly more efficient and stable than EPSDE in high dimensional problems.

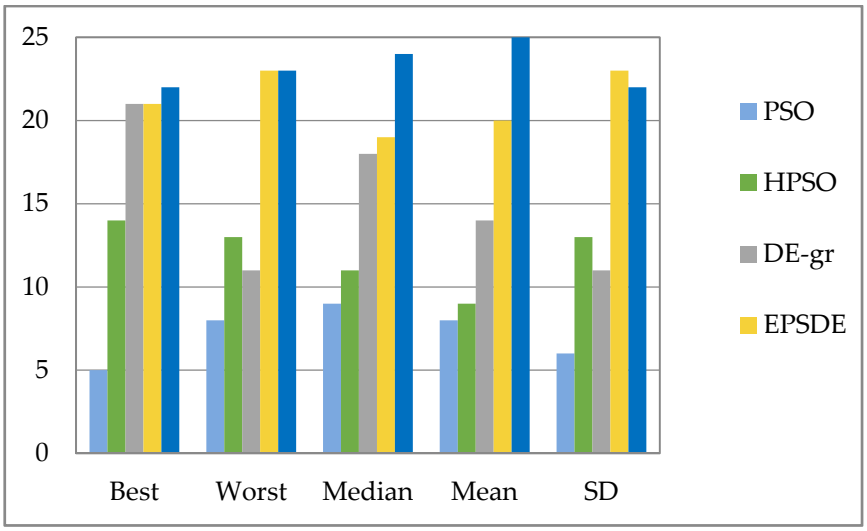

Figure 23. The statistical values of the five metaheuristic optimization methods.

6. Conclusions

Metaheuristic optimization methods are developing rapidly and have been widely applied to numerous optimization design problems, such as the optimum dimensional synthesis of the path-generating four-bar linkages in this study. However, the selection of an accurate, effective, and fast converge optimization method is still worth exploring. This research comparatively studies the exploration and efficiency of five selected metaheuristic optimization methods, including two swarm intelligence-based algorithms (PSO and HPSO) and three evolutionary-based algorithms (DE-gr, EPSDE, and L-EPSDE), which are widely used and are easily implemented metaheuristic optimization methods, by performing five representative synthesis problems of path-generating four-bar linkages. The five representative problems (three examples with prescribed timing and two examples without prescribed timing) were investigated using 100 experimental trails, in which each has a maximum iteration of 1000 (except Case 4, which has 2000). The accuracy and efficiency of the five metaheuristic methods were compared through the statistical analyses of the extensive optimal results and were also compared to those of previously reported algorithms in the literature. The results revealed that the five metaheuristic methods employed in this study can only require the execution of several optimization iterations and effectively converge to a global optimal solution of the dimensional synthesis problems of path-generating four-bar linkages. In summary, both the adaptive EPSDE and L-EPSDE methods outperformed the PSO, HPSO, and DE-gr methods and some previous algorithms presented in literature with higher accuracy (lower mean values) and efficiency (lower SDs). In addition, L-EPSDE outperformed EPSDE in the high dimensional problem owing to its ability to linearly reduce the population size in the next generation. However, DE-gr (the golden ratio numbers were selected as the parameters of the cross rate and mutation factor) exhibited similar outperforming characteristics such as EPSDE and L-EPSDE in the middle dimensional problem, and HPSO exhibited improved accuracy and efficiency than that of PSO method. Moreover, the HPSO, EPSDE, and L-EPSDE methods are potential applications in complicated middle or high dimensional optimization problems, such as the optimum dimensional synthesis of path-generating six-bar or eight-bar linkages.

Author Contributions: Y.-H.K.: Conceptualization, methodology, validation, investigation, resources, writing—original draft preparation, writing—review and editing, supervision. J.-W.L.: Investigation, writing—review and editing, supervision. W.-C.Y.: Software, data curation, validation, formal analysis. All authors have read and agreed to the published version of the manuscript.

Funding: This research received no external funding.

Institutional Review Board Statement: Not applicable.

Informed Consent Statement: Not applicable.

Data Availability Statement: Not applicable.

Conflicts of Interest: The authors declare no conflict of interest.

References

1. Payvandy, P.; Sbrahimi, S. Optimization of the thread take-up lever mechanism in lockstitch sewing machine using the imperialistic competitive algorithm. *J. Text. Polym.* **2015**, *3*, 12–19.
2. Felezi, M.E.; Vahabi, S.; Nariman-zadeh, N. Pareto optimal design of reconfigurable rice seedling transplanting mechanisms using multi-objective genetic algorithm. *Neural Comput. Appl.* **2016**, *27*, 1907–1916. [CrossRef]
3. Ji, Z.M.; Manna, Y. Synthesis of a pattern generation mechanism for gait rehabilitation. *ASME J. Med. Devices* **2008**, *2*, 031004. [CrossRef]
4. Singh, R.; Chaudhary, H.; Singh, A.K. A novel gait-based synthesis procedure for the design of 4-bar exoskeleton with natural trajectories. *J. Orthop. Transl.* **2018**, *12*, 6–15. [CrossRef]
5. Jin, S.; Kim, J.; Bae, J.; Seo, T.; Kim, J. Design, modeling and optimization of an underwater manipulator with four-bar mechanism and compliant linkage. *J. Mech. Sci. Technol.* **2016**, *30*, 4337–4343. [CrossRef]
6. Pertuz, S.A.; Llanos, C.H.; Muñoz, D.M. Development of a robotic hand using bioinspired optimization for mechanical and control design: UnB-Hand. *IEEE Access* **2021**, *9*, 61010–61023. [CrossRef]
7. Sandor, G.N.; Erdman, A.G. *Advanced Mechanism Design: Analysis and Synthesis*; Prentice-Hall Book Company: Englewood Cliffs, NJ, USA, 1984; Volume 2.
8. Fox, R.L.; Gupta, K.C. Optimization technology as applied to mechanism design. *ASME J. Eng. Ind.* **1973**, *95*, 657–663. [CrossRef]
9. Root, R.R.; Ragsdell, K.M. A survey of optimization methods applied to the design of mechanisms. *ASME J. Eng. Ind.* **1976**, *98*, 1036–1041. [CrossRef]
10. Lee, W.T.; Russell, K. Developments in quantitative dimensional synthesis (1970–2018): Four-bar path and function generation. *Inverse Probl. Sci. Eng.* **2018**, *26*, 1280–1304. [CrossRef]
11. Jensen, P.W. Synthesis of four-bar linkages with a coupler point passing through 12 points. *Mech. Mach. Theory* **1984**, *19*, 149–156. [CrossRef]
12. Tsai, L.W.; Lu, J.J. Coupler-point-curve synthesis using homotopy methods. *ASME J. Mech. Des.* **1990**, *112*, 384–389. [CrossRef]
13. Subbian, T.; Flugrad, D.R., Jr. Four-bar path generation synthesis by a continuation method. *ASME J. Mech. Des.* **1991**, *113*, 63–69. [CrossRef]
14. Wampler, C.W.; Morgan, A.P.; Sommese, A.J. Complete solution of the nine-point path synthesis problem for four-bar linkages. *ASME J. Mech. Des.* **1992**, *114*, 153–159. [CrossRef]
15. Angeles, J.; Alivizators, A.; Akhras, R. An unconstrained nonlinear least-square method of optimization of RRRR planar path generators. *Mech. Mach. Theory* **1988**, *23*, 343–353. [CrossRef]
16. Bakthavachalam, N.; Kimbrell, J.T. Optimum synthesis of path-generating four-bar mechanisms. *ASME J. Eng. Ind.* **1975**, *97*, 314–321. [CrossRef]
17. Mariappan, J.; Krishnamurty, S. A generalized exact gradient method for mechanism synthesis. *Mech. Mach. Theory* **1996**, *31*, 413–421. [CrossRef]
18. Sancibrain, R.; Viadero, F.; Garcia, P.; Fernandez, A. Gradient-based optimization of path synthesis problems in planar mechanisms. *Mech. Mach. Theory* **2004**, *39*, 839–856. [CrossRef]
19. Sancibrian, R.; García, P.; Viadero, F. A general procedure based on exact gradient determination in dimensional synthesis of planar mechanisms. *Mech. Mach. Theory* **2006**, *41*, 212–229. [CrossRef]
20. Hernández, A.; Muñoyerro, A.; Urízar, M.; Amezua, E. Comprehensive approach for the dimensional synthesis of a four-bar linkage based on path assessment and reformulating the error function. *Mech. Mach. Theory* **2021**, *156*, 140126. [CrossRef]
21. Smaili, A.; Diab, N. Optimum synthesis of mechanism using tabu-gradient search algorithms. *ASME J. Mech. Des.* **2005**, *127*, 917–923. [CrossRef]
22. Smaili, A.; Diab, N. Optimum synthesis of hybrid-task mechanisms using ant-gradient search method. *Mech. Mach. Theory* **2007**, *42*, 115–130. [CrossRef]
23. Smaili, A.; Diab, N. A new approach to shape optimization for closed path synthesis of planar mechanisms. *ASME J. Mech. Des.* **2007**, *129*, 941–948. [CrossRef]
24. Diab, N.; Smaili, A. Optimum exact/approximated point synthesis of planar mechanisms. *Mech. Mach. Theory* **2008**, *43*, 1610–1624. [CrossRef]
25. De Bustos, I.F.; Urkullu, G.; Marina, V.G.; Ansola, R. Optimization of planar mechanisms by using a minimum distance function. *Mech. Mach. Theory* **2019**, *138*, 149–168. [CrossRef]
26. Kennedy, J.; Eberhart, R.C. Particle swarm optimization. In Proceedings of the International Conference on Neural Networks, Perth, WA, Australia, 27 November–1 December 1995; Volume 4, pp. 1942–1948.

27. Yang, X.S.; Deb, S. Cuckoo search via L´evy flights. In Proceedings of the World Congress on Nature & Biologically Inspired Computing, Coimbatore, India, 9–11 December 2009; pp. 210–214.
28. Gandomi, A.H.; Alavi, H. Krill herd: A new bio-inspired optimization algorithm. *Commun. Nonlinear Sci. Numer. Simul.* **2012**, *17*, 4831–4845. [CrossRef]
29. Holland, J.H. *Adaptation in Natural and Artificial Systems*; The University of Michigan Press: Ann Arbor, WA, USA, 1975.
30. Storn, R.; Price, K. Differential evolution- a simple and efficient heuristic for global optimization over continuous spaces. *J. Glob. Optim.* **1997**, *11*, 341–359. [CrossRef]
31. Atashpaz-Gargari, E.; Lucas, C. Imperialist competitive algorithm: An algorithm for optimization inspired by imperialistic competition. In Proceedings of the 2007 IEEE Congress on Evolutionary Computation, Singapore, 25–28 September 2007; pp. 4661–4667.
32. Rao, R.V.; Savsani, V.J.; Vakharia, D.P. Teaching-learning-based optimization: A novel method for constrained mechanical design optimization problems. *Comput.-Aided Des.* **2011**, *43*, 303–315. [CrossRef]
33. Kang, Y.H.; Lee, C.T. The synthesis of four-bar linkages for path generation using hybrid particle swarm optimization. In Proceedings of the First IFToMM Asian Conference on Mechanism and Machine Science, Taipei, Taiwan, 21–25 October 2010; pp. 1–8.
34. Bulatovic, R.R.; Miodragovic, C.; Boskovic, M.S. Modified krill herd (MKH) algorithm and its application in dimensional synthesis of a four-bar linkage. *Mech. Mach. Theory* **2016**, *95*, 1–21. [CrossRef]
35. Lin, W.Y.; Hsiao, K.M. Cuckoo search and teaching-learning-based optimization for optimum synthesis of path-generating four-bar mechanisms. *J. Chin. Inst. Eng.* **2017**, *40*, 6–74. [CrossRef]
36. Sadeghi, S.M.; Bakhshinezhad, N.; Fathi, A.; Daniali, H.M. An optimal defect-free of four-bar mechanisms using constrained APT-FPSO algorithm. *J. Comput. Robot.* **2019**, *12*, 39–48.
37. Mo, X.; Ge, W.; Zhao, D.; Shen, Y. Path and function synthesis of multi-bar mechanisms using beetle antennae search algorithm. *Filomat* **2020**, *34*, 5215–5233. [CrossRef]
38. Connor, A.M.; Douglas, S.; Gilmartin, M. The kinematic synthesis of path generating mechanisms using genetic algorithms. In Proceedings of the 10th International Conference on Applications of Artificial Intelligence in Engineering, Udine, Italy, 4–6 July 1995; pp. 237–244.
39. Kunjur, A.; Krishnamurty, S. Genetic algorithms in mechanism synthesis. *J. Appl. Mech. Robot.* **1997**, *4*, 18–24.
40. Zhou, H.; Cheung, E.H.M. Optimal synthesis of crank-rocker linkages for path generation using the orientation structural error of the fixed link. *Mech. Mach. Theory* **2001**, *36*, 973–982. [CrossRef]
41. Cabrera, J.A.; Simon, A.; Prado, M. Optimal synthesis of mechanisms with genetic algorithms. *Mech. Mach. Theory* **2002**, *37*, 1165–1177. [CrossRef]
42. Shiakolas, P.S.; Koladiya, D.; Keberle, J. On the optimum synthesis of four-bar linkage using differential envolution and the geometric centroid of precision positions. *Inv. Probl. Eng.* **2002**, *10*, 485–502. [CrossRef]
43. Laribi, M.A.; Mlika, A.; Romdhane, L.; Zegloul, S. A combined genetic algorithm-fuzzy logic method (GA-FL) in mechanism synthesis. *Mech. Mach. Theory* **2004**, *39*, 717–735. [CrossRef]
44. Nariman-Zadeh, N.; Felezi, M.; Jamali, A.; Ganji, M. Pareto optimal synthesis of four-bar mechanisms for path generation. *Mech. Mach. Theory* **2009**, *44*, 180–191. [CrossRef]
45. Bulatović, R.R.; Dordević, S.R. On the optimal synthesis of a four-bar linkage using differential evolution and method of variable controlled deviations. *Mech. Mach. Theory* **2009**, *44*, 235–246. [CrossRef]
46. Acharyya, S.K.; Mandal, M. Performance of EAs for four-bar linkage synthesis. *Mech. Mach. Theory* **2009**, *44*, 1784–1794. [CrossRef]
47. Lin, W.Y. A GA-DE hybrid evolutionary algorithm for path synthesis of four-bar linkage. *Mech. Mach. Theory* **2010**, *45*, 1096–1107. [CrossRef]
48. Cabrera, J.A.; Ortiz, A.; Nadal, F.; Castillo, J.J. An evolutionary algorithm for path synthesis of mechanisms. *Mech. Mach. Theory* **2011**, *46*, 127–141. [CrossRef]
49. Peñuñuri, F.; Peón-Escalante, R.; Villanueva, C.; Pech-Oy, D. Synthesis of mechanisms for single and hybrid tasks using differential evolution. *Mech. Mach. Theory* **2011**, *46*, 1135–1349.
50. Khorshidi, M.; Soheilypour, M.; Peyro, M.; Atai, A.; Panahi, M.S. Optimal design of four-bar mechanisms using hybrid multi-objective GA with adaptive local search. *Mech. Mach. Theory* **2011**, *46*, 1453–1465. [CrossRef]
51. Matekar, S.B.; Gogate, G.R. Optimum synthesis of path generating four-bar mechanisms using differential evolution and a modified error function. *Mech. Mach. Theory* **2012**, *52*, 58–179. [CrossRef]
52. Badduri, J.; Srivatsan, R.A.; Kumar, G.S.; Bandyopadhyay, S. Coupler-curve synthesis of a planar four-bar mechanism using NSGA-II. In *Simulated Evolution and Learning*; Lecture Notes on Computer Science; Springer: Berlin/Heidelberg, Germany, 2012; Volume 7673, pp. 460–469.
53. Ortiz, A.; Cabrera, J.A.; Nadal, F.; Bonilla, A. Dimensional synthesis of mechanisms using differential evolution with auto-adaptive control parameters. *Mech. Mach. Theory* **2013**, *64*, 210–229. [CrossRef]
54. Lin, W.Y. Optimization of scale-rotation-translation synthesis after shape synthesis for path generation of planar mechanisms. *J. Chin. Inst. Eng.* **2014**, *37*, 497–505. [CrossRef]
55. Ebrahimi, S.; Payvandy, P. Efficiency constrained synthesis of path generating four-bar mechanisms based on the heuristic optimization algorithms. *Mech. Mach. Theory* **2015**, *85*, 189–204. [CrossRef]

56. Lin, W.Y.; Hsiao, K.M. More effective optimum synthesis of path generating four-bar mechanisms. *J. Multidiscip. Eng. Sci. Technol.* **2015**, *2*, 905–913.
57. Hernandez-Ocana, B.; Pozos-Parra, M.D.P.; Mezura-Montes, E.; Portilla-Flores, E.A.; Vega-Alvarado, E.; Calva-Yanez, M.B. Two-swin operators in the modified bacterial foraging algorithm for the optimal synthesis of four-bar mechanisms. *Comput. Intell. Neurosci.* **2016**, *2016*, 4525294. [CrossRef]
58. Sleesongsom, S.; Bureerat, S. Four-bar linkage path generation through self-adaptive population size teaching-learning based optimization. *Knowl. Based Syst.* **2017**, *35*, 180–191. [CrossRef]
59. Mohamed, N.; Bilel, N.; Zouhaier, A.; Lotfi, R. Multi-objective design optimisation of four-bar mechanisms using a hybrid ICA-GA algorithm. *Intern. J. Reason.-Based Intell. Syst.* **2017**, *9*, 43–51. [CrossRef]
60. Lin, W.Y.; Hsiao, K.M. A new differential evolution algorithm with a combined mutation strategy for optimum synthesis of path-generating four-bar mechanisms. *Proc. Inst. Mech. Eng. Part C J. Mech. Eng. Sci.* **2017**, *231*, 2690–2705. [CrossRef]
61. Kafash, S.H.; Nahvi, A. Optimal synthesis of four-bar path generator linkages using circular proximity function. *Mech. Mach. Theory* **2017**, *115*, 18–34. [CrossRef]
62. Singh, R.; Chaudhary, H.; Singh, A.K. Defect-free optimal synthesis of crank-rocker linkage using nature-inspired optimization algorithms. *Mech. Mach. Theory* **2017**, *116*, 105–122. [CrossRef]
63. Buskiewicz, J. Reduced number of design parameters in optimal path synthesis with timing of four-bar linkage. *J. Theor. Appl. Mech.* **2018**, *56*, 43–55. [CrossRef]
64. Sleesongsom, S.; Bureerat, S. Optimal synthesis of four-bar linkage path generation through evolutionary computation with a novel constraint handing technique. *Comput. Intell. Neurosci.* **2018**, *2018*, 5462563. [CrossRef] [PubMed]
65. Sabaapour, M.Z.; Yoon, J.W. A novel method for optimal path synthesis of mechanisms based on tracking control of shadow robot. *Mech. Mach. Theory* **2019**, *131*, 218–233. [CrossRef]
66. Zhang, K.; Huang, Q.J.; Zhang, Y.M.; Song, J.C.; Shi, J. Hybrid Lagrange interpolation differential evolution algorithm for path synthesis. *Mech. Mach. Theory* **2019**, *134*, 512–540. [CrossRef]
67. Huang, Q.J.; Zhang, K.; Song, J.C.; Zhang, Y.M.; Shi, J. Adaptive differential evolution with a Lagrange interpolation argument algorithm. *Inf. Sci.* **2019**, *472*, 180–202. [CrossRef]
68. Romero, N.N.; Campos, A.; Martins, D.; Vieira, R.S. A new approach for the optimal synthesis of four-bar path generator linkages. *SN Appl. Sci.* **2019**, *1*, 1504. [CrossRef]
69. Sancibrian, R.; Sedano, A.; Sarabia, E.G.; Blanco, J.M. Hybridizing differential evolution algorithm and local search optimization for dimensional synthesis of linkages. *Mech. Mach. Theory* **2019**, *140*, 389–412. [CrossRef]
70. Flores-Pulido, L.; Portilla-Flores, E.A.; Santiago-Valentin, E.; Veta-Alvarado, E.; Yanez, M.B.C.; Nino-Suarez, P.A. A comparative study of improved harmony search algorithm in four bar mechanisms. *IEEE Access* **2020**, *8*, 148757–148778. [CrossRef]
71. Zarkandi, S. A novel optimization-based method to find multiple solutions for path synthesis of planar four-bar and slider-crank mechanisms. *Proc. Inst. Mech. Eng. Part C J. Mech. Eng. Sci.* **2021**, *235*, 5385–5405. [CrossRef]
72. Zhang, K.; Zhu, J.H.; Zhang, Y.M.; Huang, Q.J. Optimization method for linear constraint problems. *J. Comput. Sci.* **2021**, *51*, 101315. [CrossRef]
73. Bureerat, S.; Sleesongsom, S. Constraint handling technique for four-bar linkage path generation using self-adaptive teaching-learning-based optimization with a diversity archive. *Eng. Optim.* **2021**, *53*, 513–530. [CrossRef]
74. Sardashti, A.; Daniali, H.M.; Varedi-Koulaei, S.M. Geometrical similarity error function-innovative adaptive algorithm methodology in path generation synthesis of the four-bar mechanism using metaheuristic algorithms. *Proc. Inst. Mech. Eng. Part C J. Mech. Eng. Sci.* **2022**, *236*, 1550–1570. [CrossRef]
75. Valencia-Segura, L.E.; Villarreal-Cervantes, M.G.; Corona-Ramirez, L.G.; Cuenca-Jimenez, F.; Castro-Medina, A.R. Optimal synthesis of four-bar mechanism by using relative angle method: A comparative performance study. *IEEE Access* **2021**, *9*, 132990–133010. [CrossRef]
76. Huang, Q.J.; Yu, Y.H.; Zhang, K.; Li, S.Q.; Lu, H.B. Optimal synthesis of mechanisms using repellency evolutionary algorithm. *Knowl.-Based Syst.* **2022**, *239*, 107928. [CrossRef]
77. Sy, N.V.; Lieu, Q.X.; Nguyen, X.M.; Nguyen, T.T.N. A new study on optimization of four-bar mechanisms based on a hybrid-combined differential evolution and Jaya algorithm. *Symmetry* **2022**, *14*, 381.
78. Yao, X.Y.; Wang, X.D.; Sun, W.; Kong, J.Y.; Lin, Z.K. Optimal synthesis of four-bar linkages for path generation using the individual repairing method. *Mech. Sci.* **2022**, *13*, 79–87. [CrossRef]
79. McGarva, J.R. Rapid search and selection of path generation mechanisms from a library. *Mech. Mach. Theory* **1994**, *29*, 223–235. [CrossRef]
80. Ullah, I.; Kota, S. Optimal Synthesis of mechanism for path generation using Fourier descriptors and global search methods. *ASME J. Mech. Des.* **1997**, *119*, 504–510. [CrossRef]
81. Vasiliu, A.; Yannou, B. Dimensional synthesis of planar mechanisms using neural networks: Application to path generator linkages. *Mech. Mach. Theory* **2001**, *36*, 299–310. [CrossRef]
82. Liu, Y.; Xiao, R. Optimal synthesis of mechanisms for path generation using refined numerical representation based model and AIS based searching method. *ASME J. Mech. Des.* **2005**, *127*, 688–691. [CrossRef]
83. Starosta, R. Application of genetic algorithm and Fourier coefficients (GA-FC) in mechanism synthesis. *J. Theor. Appl. Mech.* **2008**, *46*, 395–411.

84. Galán-Marín, G.; Alonso, F.J.; Del Castillo, J.M. Shape optimization for path synthesis of crank-rocker mechanisms using a wavelet-based neural network. *Mech. Mach. Theory* **2009**, *44*, 1132–1143. [CrossRef]
85. Buskiewicz, J.; Starosta, R.; Walczak, T. On the application of curve curvature in path synthesis. *Mech. Mach. Theory* **2009**, *44*, 1223–1239. [CrossRef]
86. Khan, N.; Ullah, I.; Al-Grafi, M. Dimensional synthesis of mechanical linkages using artificial neural networks and Fourier descriptors. *Mech. Sci.* **2015**, *6*, 29–34. [CrossRef]
87. Sun, J.; Liu, W.; Chu, J. Dimensional synthesis of open path generator of four-bar mechanisms using the Haar wavelet. *ASME J. Mech. Des.* **2015**, *137*, 082303. [CrossRef]
88. Lin, X.Y.; Chen, P. A parameterization-invariant Fourier approach to planar linkage synthesis for path generation. *Math. Probl. Eng.* **2017**, *2017*, 8458149.
89. Sharma, S.; Purwar, A.; Ge, Q.J. An optimal parametrization scheme for path generation using Fourier descriptors for four-bar mechanism synthesis. *ASME J. Comput. Inf. Sci. Eng.* **2019**, *19*, 014501. [CrossRef]
90. Kim, J.-W.; Seo, T.; Kim, J. A new design methodology for four-bar linkage mechanisms based on derivations of coupler curve. *Mech. Mach. Theory* **2016**, *100*, 138–154. [CrossRef]
91. Kim, J.-W.; Jeong, S.M.; Kim, J.; Seo, T.W. Numerical hybrid Taguchi-random coordinate search algorithm for path synthesis. *Mech. Mach. Theory* **2016**, *102*, 203–216. [CrossRef]
92. Li, X.G.; Wei, S.M.; Liao, Q.H.; Zhang, Y. A novel analytical method for the four-bar path generation synthesis based on Fourier series. *Mech. Mach. Theory* **2020**, *144*, 103671. [CrossRef]
93. Ahmadi, B.; Nariman-Zadeh, N.; Jamali, A. A Stackelberg game theoretic multi-objective synthesis of four-bar mechanisms. *Struct. Multidiscipl. Optim.* **2019**, *60*, 699–710. [CrossRef]
94. Ahmadi, B.; Ahmadi, B.; Chegini, S.N. Multi-objective reliability-based optimal synthesis of path generating four-bar mechanisms: A cooperative game theoretic approach. *Proc. Inst. Mech. Eng. Part C J. Mech. Eng. Sci.* **2022**, *236*, 2298–2311. [CrossRef]
95. Mallipeddi, R.; Suganthan, P.N.; Pan, Q.K.; Tasgetiren, M.F. Differential evolution algorithm with ensemble of parameters and mutation strategies. *Appl. Soft Comput.* **2011**, *11*, 1679–1696. [CrossRef]
96. Shi, Y.H.; Eberhart, R.C. A modified particle swarm optimizer. In Proceedings of the IEEE 1998 International Conference on Evolutionary Computation, Anchorage, AK, USA, 4–9 May 1998; pp. 69–73.
97. Clerc, M. The swarm and the queen: Towards a deterministic and adaptive particle swarm optimization. In Proceedings of the 1999 Congress on Evolutionary Computation, Washington, DC, USA, 6–9 July 1999; Volume 3, pp. 1951–1957.
98. Tanabe, R.; Fukunaga, A.S. Improving the search performance of SHADE using linear population size reduction. In Proceedings of the IEEE Congress on Evolutionary Computation, Beijing, China, 6–11 July 2014; pp. 1658–1665.
99. Yan, H.S.; Wu, L.I.; Hwang, W.M.; Wu, Y.C.; Lan, C.C. *Modern Mechanisms*; Dong-Hua Book Company: Taiwan, China, 2021. (In Chinese)